



doi:10.1016/S0016-7037(00)00094-2

## The age of Dar al Gani 476 and the differentiation history of the martian meteorites inferred from their radiogenic isotopic systematics

LARS E. BORG,<sup>1,\*</sup> LARRY E. NYQUIST,<sup>2</sup> HENRY WIESMANN,<sup>3</sup> CHI-YU SHIH,<sup>3</sup> and YOUNG REESE<sup>3</sup><sup>1</sup>Institute of Meteoritics, University of New Mexico, Albuquerque, NM 87131, USA<sup>2</sup>SN2/NASA Johnson Space Center, Houston, TX 77058, USA<sup>3</sup>Lockheed Engineering and Science Co., 2400 NASA Road, Houston, TX 77258, USA

(Received July 1, 2002; accepted in revised form December 18, 2002)

**Abstract**—Samarium–neodymium isotopic analysis of the martian meteorite Dar al Gani 476 yields a crystallization age of  $474 \pm 11$  Ma and an initial  $\epsilon_{\text{Nd}}^{143}$  value of  $+36.6 \pm 0.8$ . Although the Rb–Sr isotopic system has been disturbed by terrestrial weathering, and therefore yields no age information, an initial  $^{87}\text{Sr}/^{86}\text{Sr}$  ratio of  $0.701249 \pm 33$  has been estimated using the Rb–Sr isotopic composition of the maskelynite mineral fraction and the Sm–Nd age. The Sr and Nd isotopic systematics of Dar al Gani 476, like those of the basaltic shergottite QUE94201, are consistent with derivation from a source region that was strongly depleted in incompatible elements early in the history of the solar system. Nevertheless, Dar al Gani 476 is derived from a source region that has a slightly greater incompatible enrichment than the QUE94201 source region. This is not consistent with the fact that the parental magma of Dar al Gani 476 is significantly more mafic than the parental magma of QUE94201, and underscores a decoupling between the major element and trace element–isotopic systematics observed in the martian meteorite suite.

Combining the  $\epsilon_{\text{Nd}}^{142}$ – $\epsilon_{\text{Nd}}^{143}$  isotopic systematics of the martian meteorites yields a model age for planetary differentiation of  $4.513_{-0.033}^{+0.027}$  Ga. Using this age, the parent/daughter ratios of martian mantle sources are calculated assuming a two-stage evolutionary history. The calculated sources have very large ranges of parent/daughter ratios ( $^{87}\text{Rb}/^{86}\text{Sr} = 0.037$ – $0.374$ ;  $^{147}\text{Sm}/^{144}\text{Nd} = 0.182$ – $0.285$ ;  $^{176}\text{Lu}/^{177}\text{Hf} = 0.028$ – $0.048$ ). These ranges exceed the ranges estimated for terrestrial basalt source regions, but are very similar to those estimated for the sources of lunar mare basalts. In fact, the range of parent/daughter ratios calculated for the martian meteorite sources can be produced by mixing between end-members with compositions similar to lunar mare basalt sources. Two of the sources have compositions that are similar to olivine and pyroxene-rich mafic cumulates with variable proportions of a Rb-enriched phase, such as amphibole, whereas the third source has the composition of liquid trapped in the cumulate pile (i.e. similar to KREEP) after  $\sim 99\%$  crystallization. Correlation between the proportion of trapped liquid in the meteorite source regions and estimates of  $f_{\text{O}_2}$  suggest that the KREEP-like component may be hydrous. The success of these models in reproducing the martian meteorite source compositions suggests that the variations in trace element and isotopic compositions observed in the martian meteorites primarily reflect melting of the crystallization products of an ancient magma ocean, and that assimilation of evolved crust by mantle derived magmas is not required. Furthermore, the decoupling of major element and trace element–isotopic systematics in the martian meteorite suite may reflect the fact that trace element and isotopic systematics are inherited from the magma source regions, whereas the major element abundances are limited by eutectic melting processes at the time of magma formation. Differences in major element abundances of parental magma, therefore, result primarily from fractional crystallization after leaving their source regions. Copyright © 2003 Elsevier Ltd

### 1. INTRODUCTION

The compositions of martian meteorites are paradoxical because, on one hand, the parental magmas are basaltic in composition (Stolper and McSween, 1979; Treiman, 1986; McSween et al., 1988, 1996; Longhi and Pan, 1989; Harvey et al., 1993) and therefore have a limited range of major element abundances, whereas on the other hand, they display a very large range of trace element abundances and isotopic compositions. In fact, initial Sr and Nd isotopic compositions determined on nine basaltic shergottites define a greater range than almost all terrestrial basalts (Borg et al., 2002). Various trace-element and isotope-based models suggest that the compositional variability observed in the martian meteorites is the result

of a mixing processes (e.g., Shih et al., 1982; Jones, 1989; Borg et al., 1997a,b, 2002). The incompatible-element depleted end of the mixing array is constrained by meteorites that are characterized by light-rare-earth element (LREE) depleted REE patterns (Fig. 1), and low initial Sr and high initial Nd isotopic compositions. The evolved end of the array is more poorly constrained, but is thought to be either martian crust (e.g., Jones, 1989; Borg et al., 1997a; Herd et al., 2002) or an enriched component in the martian mantle (e.g., Borg et al., 1997b, 2002; Brandon et al., 2000). In either case, the fact that the martian meteorites define a whole rock Rb–Sr isochron with an age of  $\sim 4.5$  Ga require these reservoirs to have formed near the time of planet formation and to have remained isolated until just before the time of crystallization of the meteorites (e.g., Shih et al., 1982).

The basaltic shergottite QUE94201 (QUE) has bulk rock La/Yb ratio of  $\sim 0.1$ , an initial  $^{87}\text{Sr}/^{86}\text{Sr}$  ratio of 0.7013, and

\* Author to whom correspondence should be addressed (lborg@unm.edu).

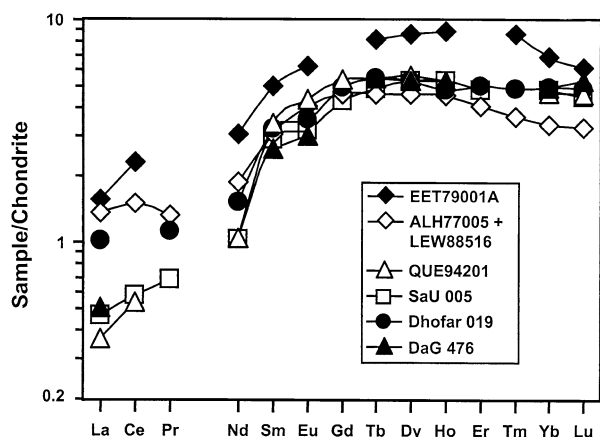


Fig. 1. Chondrite-normalized rare earth element plot of LREE-depleted martian meteorites DaG 476, Dhofar 019, SaU 005, QUE94201, ALH77005/LEW88516, and EET79001A. Normalization to values of Anders and Grevesse (1989). Data from Ma et al. (1982), Shih et al. (1982), Burgele et al. (1983), Dreibus et al. (1992, 1996, 2000), Taylor et al. (2002), Zipfel et al. (2000).

initial  $\epsilon_{\text{Nd}}^{143}$  value of +48 (Borg et al., 1997b). Although this rock has trace element and isotopic systematics that are characteristic of depleted martian mantle, it has an evolved parental magma composition (Mg# of  $\sim 38$ ; McSween et al., 1996). Dar al Gani 476 (DaG) has a REE pattern that is very similar to QUE (Fig. 1), but has a parental magma composition that is significantly more Mg-rich (Mg#  $\sim 68$ ). In fact, DaG is one of the most mafic basaltic shergottites found so far (Zipfel et al., 2000). Thus, the Sr and Nd isotopic analysis of DaG is expected to place additional constraints on the isotopic composition of martian mantle source regions, as well as help define the relationship between Sr and Nd isotopic compositions and parental magma compositions. These relationships can be used to constrain the processes responsible for the variations in the trace-element and isotopic compositions of the martian meteorite suite. The goals of this study are to: (1) determine the age and initial Sr and Nd isotopic compositions of DaG, (2) better constrain the range of depleted martian mantle isotopic compositions, (3) better define the age of mantle depletion, and hence planetary differentiation, on Mars, and (4) determine the relationship of DaG to the other martian meteorites.

## 2. PETROLOGY AND COMPOSITION OF DAR AL GANI 476

Dar al Gani 476 is a basaltic shergottite that was found in the Saharan desert in Libya in 1998, and has been described by Zipfel et al. (2000), Mikouchi et al. (2001) and Wadhwa et al. (2001). The meteorite has a porphyritic texture in which a fine grained ground mass of clinopyroxene and maskelynite surround euhedral to subhedral megacrysts of olivine and orthopyroxene. The olivine megacrysts range in size up to 5 mm, whereas orthopyroxene megacrysts are smaller and average approximately 0.3 mm in size. Dar al Gani contains approximately 58–65% pyroxene, 10–24% olivine, 12–17% maskelynite, with minor amounts of chromite, ilmenite, sulfides and phosphates. The pyroxene consists primarily of pigeonite, although 1–13% of the mode is orthopyroxene and augite. In

addition to these igneous phases, DaG contains approximately 4–7% impact melt glass and 2–3% secondary alteration products.

Secondary alteration products in DaG include: calcite, gypsum, barite, an amorphous silica phase, and phyllosilicates (Crozz and Wadhwa, 2001; Zipfel et al., 2000; Edmunson et al., 2001). Weathering of DaG is also manifest by its bulk rock composition. The main compositional evidence for weathering is elevated K/La ratios. The K/La ratio of DaG ranges from 2630–4610 depending on how near the analyzed aliquot was from the surface of the meteorite (Zipfel et al., 2000). These ratios are higher than both Antarctic shergottites (560–1200) and other basaltic shergottites from desert environments such as SaU 005 and Dhofar 019 (1465–1770; Dreibus et al., 2000; Taylor et al., 2002). Comparison of samples derived from the interior and exterior portions of DaG led Zipfel et al. (2000) to conclude that K, Ca, Ba, As, and U were added to the sample by weathering in a hot desert environment, whereas REE were not.

The DaG pyroxenes and olivines have high Mg#'s indicating that it is one of the most mafic basaltic shergottites (Zipfel et al., 2000; Mikouchi et al., 2001; Wadhwa et al., 2001). The Mg# of DaG is 68 and is only slightly lower than the Mg#'s of 70–71 of the lherzolitic shergottites (Banin et al., 1992; Dreibus et al., 1992). Although DaG and the lherzolitic shergottites are cumulates, the relatively high Mg#'s of their whole rocks and mafic silicates, suggest that these meteorites have undergone minimal amounts of differentiation. This is supported by low incompatible element abundances in DaG relative to the other shergottites. The measured whole rock La abundance is 0.09–0.12 ppm, whereas the Yb abundance is 0.73–0.81 ppm (Zipfel et al., 2000). Therefore, the whole rock REE pattern for DaG is very strongly depleted in LREE (Fig. 1). In conclusion, DaG appears to have undergone a relatively minor amount of differentiation since leaving its mantle source region, and be derived from a source that is strongly depleted in incompatible elements. Thus, DaG probably has an isotopic composition that reflects the composition of its mantle source region.

## 3. ANALYTICAL TECHNIQUES

The mineral separation and leaching procedures were designed according to two observations. First, preliminary petrographic examination of DaG led to the conclusion that the extremely large size of the olivine megacrysts could indicate a xenocrystic origin (Mikouchi, 1999). As a result, the mineral separation procedure needed to completely separate the olivine megacrysts from the finer grained ground mass. Second, DaG has been extensively weathered in the Libyan desert (e.g., Crozz and Wadhwa, 2001) so that the leaching procedures needed to remove as much terrestrial secondary alteration as possible.

The mineral separation procedure is presented in Figure 2. An initial 1.3 g sample of DaG was coarsely crushed in a boron carbide mortar and pestle and then sieved at 500  $\mu\text{m}$ . Aliquots of this material were dispensed to D. Bogard and D. Mittlefehldt for noble gas and neutron activation analysis, leaving 640 mg for Rb-Sr and Sm-Nd chronology studies. The remaining 640 mg sample was sieved at 44  $\mu\text{m}$  to remove the finest material. From the 44–500  $\mu\text{m}$  material, the large olivine megacrysts were removed by hand-picking with tweezers. This was a fairly efficient process because the olivines were not easily crushed and yielded a 109 mg olivine separate. The olivine yield represented  $\sim 17\%$  of the sample and was consistent with petrographic estimates of the olivine mode (10–24%). The olivine megacrysts were leached in an ultrasonic bath in 2N HCl at 25°C for 10 minutes. The remaining sample, consisting primarily of pyroxene and maskelynite, was crushed

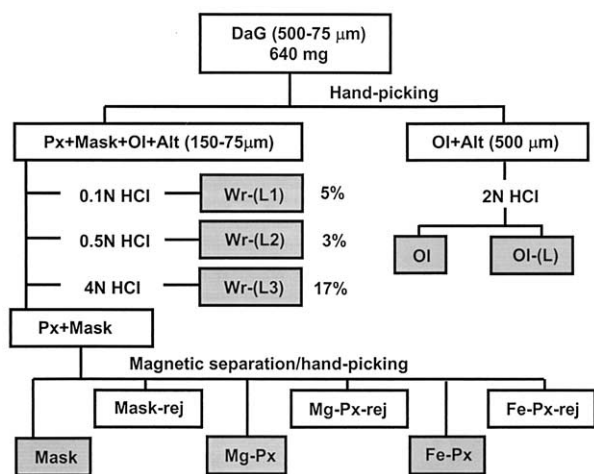


Fig. 2. Schematic representation of the mineral separation procedure used in this study for Dar al Gani 476. Shaded areas represent samples analyzed for Rb-Sr and Sm-Nd isotopic compositions.

to  $<150 \mu\text{m}$  and then leached in an ultrasonic bath in 0.1N, 0.5N, and 4N HCl for 10 minutes each. The 0.1N HCl leaching was completed at  $25^\circ\text{C}$ , whereas the 0.5N and the 4N HCl leaching steps were completed at  $45^\circ\text{C}$ . The sample was washed in quartz distilled water and centrifuged between leaching steps. Approximately 27.5 mg, 15.0 mg, and 88.6 mg of material were dissolved in the 0.1N, 0.5N, and 4N HCl leaching steps and represented dissolution of 5%, 3%, and 17% of the remaining sample, respectively. Microscopic examination revealed that no olivine remained in the sample after the 4N HCl leaching step. The remaining material was then sieved at  $74\text{--}150$ ,  $44\text{--}74$  and  $<44 \mu\text{m}$ . Maskelynite, Mg-rich pyroxene, and Fe-rich pyroxene were separated from the coarse ( $74\text{--}150 \mu\text{m}$ ) size fraction using the Frantz isodynamic separator. Final purification of the minerals separates was completed by hand-picking.

Both mineral fractions and leachates were analyzed for Rb-Sr and Sm-Nd isotopic compositions. Mineral fractions analyzed include: olivine (Ol), maskelynite (Mask), Mg-rich pyroxene (Mg-Px), and Fe-rich pyroxene (Fe-Px). The leachates analyzed include: the 0.1N HCl leachate (Wr-(L1)), the 0.5N HCl leachate (Wr-(L2)), the 4N HCl leachate (Wr-(L3)), and the olivine leachate (Ol-(L)). The sample digestion, chemical separation procedures, and procedural blanks were reported in Borg et al. (2002).

## 4. RESULTS

### 4.1. Sm-Nd Isochron

The results of Sm-Nd isotopic analyses are presented in Table 1 and on an isochron diagram (Fig. 3a). The Sm-Nd isotopic system yields an age of  $474 \pm 11$  Ma and an initial  $\epsilon_{\text{Nd}}^{143}$  value of  $+36.6 \pm 0.8$ . This age is defined by the maskelynite, olivine, Fe-pyroxene and Mg-pyroxene mineral fractions. This isochron yields a MSWD of 0.8, indicating a good fit of the isotopic data to the regressed isochron. The leachates are not used to define the age of DaG. Nevertheless, an age of  $459 \pm 26$  Ma is defined by all mineral and leachate fractions, indicating that the leachates lie very near the isochron defined by the mineral fractions (inset, Fig. 3a).

The leachate and pyroxene mineral fractions have  $^{147}\text{Sm}/^{144}\text{Nd}$  ratios that are similar to ratios determined by ion microprobe on phosphates and pyroxenes from DaG (Wadhwa et al., 2001). For example, Wadhwa et al. (2001) determined that merrillite in DaG has a  $^{147}\text{Sm}/^{144}\text{Nd}$  ratio of 0.47, which is in good agreement with the  $^{147}\text{Sm}/^{144}\text{Nd}$  ratios determined for the leachates (0.45–0.49). Pyroxene mineral fractions are composed of a variety of pyroxene types and therefore cannot be directly compared to ion microprobe analyses of individual pyroxene grains. However, the Sm and Nd abundances of a bulk mineral fraction calculated using the compositions and pyroxene mode (pigeonite:orthopyroxene:augite = 76:4:20) reported by Wadhwa et al. (2001) are similar to the abundances determined on our mineral fractions. The calculated Sm and Nd abundances are 0.056 ppm and 0.046 ppm, respectively, whereas the average Sm and Nd abundances of the pyroxene mineral fractions are 0.069 ppm and 0.043 ppm, respectively. The calculated  $^{147}\text{Sm}/^{144}\text{Nd}$  ratio is 0.74, which is somewhat lower than the value of  $\sim 0.95$  determined on the pyroxene mineral fractions. However, the  $^{147}\text{Sm}/^{144}\text{Nd}$  ratios, and Sm and Nd abundances calculated for the mineral fraction, are strongly dependent on the augite mode and the REE abundances in the augite. The mode of DaG determined by Zipfel et al. (2000) contained significantly less augite yielding a  $^{147}\text{Sm}/^{144}\text{Nd}$  ratio that is higher (0.83) than the ratio calculated with

Table 1. Sm-Nd isotopic analyses of Dar al Gani 476.

Fraction	wt. (mg)	Sm (ppm/nm)	Nd (ppm/nm)	$^{147}\text{Sm}/^{144}\text{Nd}^a$	$^{143}\text{Nd}/^{144}\text{Nd}^b$
Mask (R)	25.58	0.0587	0.0435	$0.81489 \pm 163$	$0.515624 \pm 26$
Olivine (R)	84.82	0.0759	0.0709	$0.64795 \pm 65$	$0.515122 \pm 11$
Fe-Px (R)	59.87	0.0683	0.0417	$0.96017 \pm 96$	$0.516110 \pm 24$
Mg-Px (R)	66.03	0.0697	0.0449	$0.93813 \pm 103$	$0.516000 \pm 29$
Wr (L1) <sup>d</sup>		(0.027)	(0.037)	$0.45455 \pm 45$	$0.514424 \pm 61$
Wr (L2) <sup>d</sup>		(0.040)	(0.053)	$0.47302 \pm 47$	$0.514543 \pm 34$
Wr (L3)		(0.037)	(0.048)	$0.49090 \pm 49$	$0.514685 \pm 24$
Olivine (L)		(0.110)	(0.146)	$0.47840 \pm 48$	$0.514673 \pm 18$
AMES Nd Std (N = 51) <sup>c</sup>					$0.511098 \pm 24$

Note. Wr = whole rock, Px = pyroxene, Mask = maskelynite, L = leachate, R = residue, ppm = parts per million for mineral fractions and whole rocks, nm = nanomoles for leachates in parentheses.

<sup>a</sup> Error limits apply to last digits and include a minimum uncertainty of 0.5% plus 50% of the blank correction for Sm and Nd added quadratically.

<sup>b</sup> Normalized to  $^{86}\text{Sr}/^{88}\text{Sr} = 0.1194$ . Uncertainties refer to last digits and are  $2\sigma_m$  calculated from the measured isotopic ratios.  $2\sigma_m = [\sum(m_i - \mu)^2 / (n(n-1))]^{1/2}$  for n ratio measurements  $m_i$  with mean value  $\mu$ .

<sup>c</sup> Uncertainties refer to last digits and are  $2\sigma_p$ .  $2\sigma_p = [\sum(M_i - \pi)^2 / (N-1)]^{1/2}$  for N measurements  $M_i$  with mean value  $\pi$ . Isochron is calculated using either  $2\sigma_p$  (from standard runs) or  $2\sigma_m$  (from measured isotopic ratios), whichever is larger.

<sup>d</sup> Run as Nd<sup>+</sup>. All other samples run as NdO<sup>+</sup>.

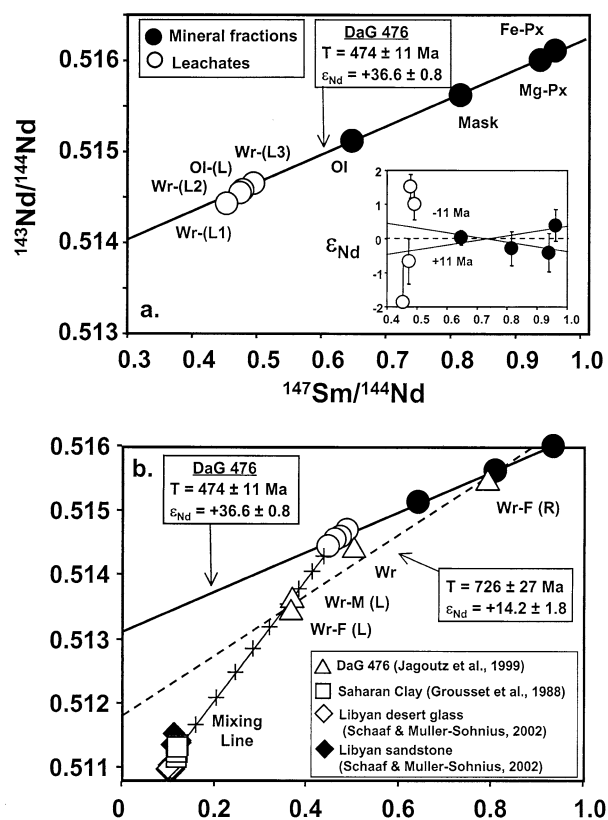


Fig. 3. Samarium-neodymium isochron plots for Dar al Gani 476. Ages calculated using the method of York (1966). (a) Isochron plot of fractions analyzed in this study. An age of  $475 \pm 11$  Ma and  $\epsilon_{Nd}^{143}$  value of  $+36.6 \pm 0.8$  is defined by the silicate mineral fractions (filled circles). Although the leachates (open circles) lie near the isochron (inset) they are not used to define the age. (b) Isochron plot of fractions analyzed in this study (circles) and by Jagoutz et al. (1999; open triangles). The composition of Saharan clays (open squares) is from Grousset et al. (1988) and the composition of Libyan desert glass (open diamonds) and sandstones (filled diamonds) from Schaaf and Müller-Sohnius (2002). Note that leachates lie on a mixing line defined by Saharan clays and igneous phosphates. The phosphate end-member is assumed to have the Sm and Nd abundances determined for phosphate by ion microprobe by Wadhwa et al. (2001) and the Nd isotopic composition of the leachates analyzed in this study. Tick marks represent 10% mixing intervals. The model suggests that the leachates completed by Jagoutz et al. (1999) contained  $\sim 40\%$  Nd derived from Saharan clays.

the mode of Wadhwa et al. (2001). Also, the  $^{147}\text{Sm}/^{144}\text{Nd}$  ratios of the augite are quite variable (0.57–1.14). Thus, there appears to be good agreement between the Sm and Nd abundances calculated for the mineral fractions and the abundances measured for the mineral fractions.

In contrast to the leachates and pyroxene mineral fractions, the maskelynite and olivine mineral fractions have Sm and Nd abundances and  $^{147}\text{Sm}/^{144}\text{Nd}$  ratios that differ substantially from the ion microprobe analyses of Wadhwa et al. (2001), as well as from values predicted from igneous partitioning (Edmunson et al., 2001). Edmunson et al. (2001), however, found numerous olivine and maskelynite grains with Sm and Nd abundances and  $^{147}\text{Sm}/^{144}\text{Nd}$  ratios similar to the mineral fractions. They speculated that the high REE abundances and low

$^{147}\text{Sm}/^{144}\text{Nd}$  ratios observed in the olivines and olivine mineral fractions could result from redistribution of melt inclusions within the olivines as a result of shock processes. Edmunson et al. (2001) also observed some melt inclusions with relatively high  $^{147}\text{Sm}/^{144}\text{Nd}$  ratios and noted that a minor contribution from inclusions with similar compositions in the maskelynite fraction could shift the  $^{147}\text{Sm}/^{144}\text{Nd}$  ratios to its measured values. Note that inclusions associated with plagioclase may have relatively high  $^{147}\text{Sm}/^{144}\text{Nd}$  ratios because they crystallized from a late-stage liquid after the stabilization of merrillite.

The age defined by the mineral fractions reported here is significantly different from the age of  $726 \pm 27$  Ma reported by Jagoutz et al. (1999). The 726 Ma age is defined by leachates and residues from whole rock samples of various sizes (Fig. 3b). The whole rock (Wr) and fine-grained whole rock residue fractions (Wr-F (R)) fall near the leachate and maskelynite mineral fractions reported here, whereas the leachates from the fine and medium-grained whole rocks, Wr-F (L) and Wr-M (L), fall below the 474 Ma isochron. The whole rock leachates of Jagoutz et al. (1999) lie on a line between the leachates reported in this study and Saharan clays analyzed by Grousset et al. (1988). Sandstone and desert glasses found in the Libyan desert have the same isotopic compositions as the clays and fall on the same line in Figure 3b (Schaaf and Müller-Sohnius, 2002). A line regressed through average Saharan clay and the leachates from both studies has a correlation coefficient ( $R^2$ ) of 0.999, suggesting that Nd from the Saharan desert soils and rocks have been incorporated into the leachates. Binary mixing models support this conclusion (Fig. 3b). One end of the mixing line is defined by the average composition of Saharan clay, whereas the other is defined by igneous phosphate. The  $^{147}\text{Sm}/^{144}\text{Nd}$  ratio used for the phosphate was determined by ion microprobe (Wadhwa et al., 2001), whereas the  $^{143}\text{Nd}/^{144}\text{Nd}$  ratio used is the average of the leachates from this study. The model indicates that 30–45% of the Nd in the leachates of Jagoutz et al. (1999) are derived from terrestrial sources.

The mixing models indicate that the proportion of Nd in the leachates derived from phosphate versus alteration products from the two studies is different. This could reflect a greater proportion of phosphate in the sample analyzed in this study. Alternatively, it could be a function of the relative freshness of the various samples analyzed for isotopic compositions. A final possibility is that the composition of the leachates is dependent on the relative grain size of the material analyzed. Our leachates were from relatively coarse grained material, whereas the leachates of Jagoutz et al. (1999) were from the finest size fractions. In this scenario, the fine-grained fractions analyzed by Jagoutz et al. (1999) contained a greater proportion of altered material.

In addition to completing a Sm-Nd isochron study, Jagoutz et al. (data reported in Brandon et al., 2000) also determined a  $\epsilon_{Nd}^{142}$  value of  $+0.75 \pm 0.29$  on a whole rock fraction. This value is similar to values measured on QUE, Chassigny, and the Nakhilites by Borg et al. (1997b) and Harper et al. (1995). The fact that the Wr fraction of Jagoutz et al. (1999) falls near the 474 Ma isochron reported here suggests that the  $\epsilon_{Nd}^{142}$  value is probably not significantly lowered by the addition of terrestrial alteration products. As a result, this value is used in a later section to constrain the age of source formation.

Table 2. Rb-Sr isotopic analyses of Dar al Gani 476.

Fraction	wt. (mg)	Rb (ppm/nm)	Sr (ppm/nm)	$^{87}\text{Rb}/^{86}\text{Sr}^a$	$^{87}\text{Sr}/^{86}\text{Sr}^b$
Mask (R)	25.58	0.208	13.55	0.04434 ± 22	0.701538 ± 12
Olivine (R)	84.82	0.410	7.728	0.15366 ± 77	0.705646 ± 18
Fe-Px (R)	59.87	0.138	3.910	0.10181 ± 51	0.703162 ± 13
Mg-Px (R)	66.03	0.143	4.664	0.08858 ± 44	0.702688 ± 14
Wr (L1)		(0.023)	(10.1)	0.00637 ± 3	0.708674 ± 18
Wr (L2)		(0.040)	(5.64)	0.01985 ± 10	0.707593 ± 15
Wr (L3)		(0.067)	(6.11)	0.03082 ± 15	0.705800 ± 16
Olivine (L)		(0.023)	(2.84)	0.02368 ± 12	0.708572 ± 12
NBS-987 (N = 46) <sup>c</sup>					0.710248 ± 27

Note. Wr = whole rock, Px = pyroxene, Mask = maskelynite, L = leachate, R = residue, ppm = parts per million for mineral fractions and whole rocks, nm = nanomoles for leachates in parentheses.

<sup>a</sup> Error limits apply to last digits and include a minimum uncertainty of 0.1% plus 50% of the blank correction for Sm and Nd added quadratically.

<sup>b</sup> Normalized to  $^{146}\text{Nd}/^{144}\text{Nd} = 0.72414$ . Uncertainties refer to last digits and are  $2\sigma_m$  calculated from the measured isotopic ratios.  $2\sigma_m = [\sum(m_i - \mu)^2 / (n(n-1))]^{1/2}$  for n ratio measurements  $m_i$  with mean value  $\mu$ .

<sup>c</sup> Uncertainties refer to last digits and are  $2\sigma_p$ ,  $2\sigma_p = [\sum(M_i - \pi)^2 / (N-1)]^{1/2}$  for N measurements  $M_i$  with mean value  $\pi$ . Isochron is calculated using either  $2\sigma_p$  (from standard runs) or  $2\sigma_m$  (from measured isotopic ratios), whichever is larger.

## 4.2. Rb-Sr Isochron

The results of Rb-Sr isotopic analyses are presented in Table 2 and on an isochron diagram (Fig. 4), but yield no age information. A line regressed through the mineral fractions has a slope corresponding to an age of  $2.6 \pm 1.4$  Ga with an initial  $^{87}\text{Sr}/^{86}\text{Sr}$  ratio near 0.7. This demonstrates that the Rb-Sr isotopic systematics of most of the mineral fractions are disturbed. The leachates also demonstrate evidence of isotopic disturbance and plot near the modern sea water  $^{87}\text{Sr}/^{86}\text{Sr}$  ratio of  $\sim 0.709$ . The leachates have Sr isotopic compositions similar

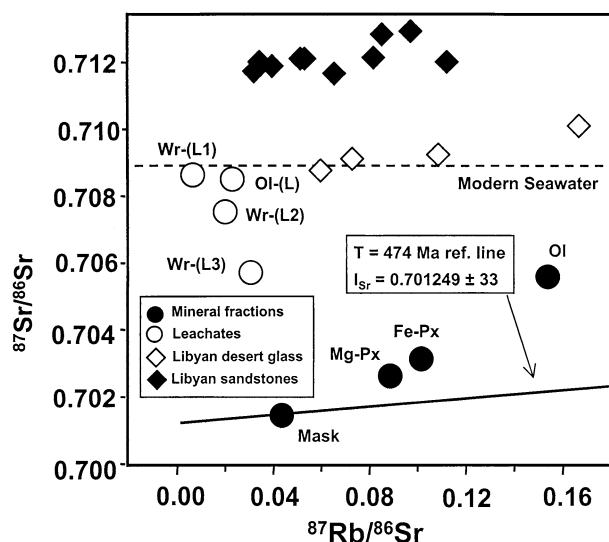


Fig. 4. Rubidium-strontium isochron plot for Dar al Gani 476. Symbols and data sources same as Figure 3. Although this plot yields no age information, and initial  $^{87}\text{Sr}/^{86}\text{Sr}$  ratio of  $0.701249 \pm 33$  for Dar al Gani 476 is defined using the maskelynite mineral fraction and the Sm-Nd age of 474 Ma. Decay constant ( $\lambda$ ) =  $0.01402 \text{ Ga}^{-1}$  (Bege-mann et al., 2001) is used in age calculations. Leachates have  $^{87}\text{Sr}/^{86}\text{Sr}$  ratios near the modern seawater value of  $\sim 0.709$ , reflecting the addition of terrestrial calcite to the meteorite. Despite leaching, the mafic silicate fractions also appear to contain terrestrial Sr as suggested by Crozaz and Wadhwa (2001).

to Libyan sandstones analyzed by Schaaf and Müller-Sohnius (2002) suggesting that rocks and soils in the Libyan desert are the ultimate source of Sr in the secondary alteration products observed in DaG. Much of the disturbance of the Rb-Sr isotopic systematics of DaG is due to formation of calcite veins in the Libyan desert. Calcite makes up approximately 2% of the mode, has a high abundance of Sr, and is easily soluble in the acids used to leach DaG. Furthermore, despite leaching in strong acids, calcite has been observed in the interiors of olivine mineral fraction grains (exposed by polishing) with a scanning electron microscope. Calcite is therefore expected to control the Sr isotopic composition of the leachates and mineral fractions. In addition, Crozaz and Wadhwa (2001) suggest that secondary alteration can add Sr to the pyroxenes and olivines, and may therefore also affect the Rb-Sr isotopic systematics of the mafic silicates in DaG, even if calcite is removed by leaching.

Although the Rb-Sr isotopic systematics of DaG appear to be disturbed through the addition of radiogenic Sr, most mineral fractions have  $^{87}\text{Sr}/^{86}\text{Sr}$  ratios that are lower than terrestrial rocks (Table 2). The  $^{87}\text{Sr}/^{86}\text{Sr}$  ratio of this source region can be estimated using the 474 Ma Sm-Nd age and the  $^{87}\text{Rb}/^{86}\text{Sr}$  and  $^{87}\text{Sr}/^{86}\text{Sr}$  ratios of the maskelynite mineral fraction. This calculation yields an initial  $^{87}\text{Sr}/^{86}\text{Sr}$  ratio for DaG of  $0.710249 \pm 33$  (Fig. 4). This represents a maximum initial  $^{87}\text{Sr}/^{86}\text{Sr}$  ratio for DaG because secondary alteration is expected to raise the  $^{87}\text{Sr}/^{86}\text{Sr}$  ratio of the maskelynite. Nevertheless, maskelynite has high abundances of Sr and therefore has a Sr isotopic composition that is less susceptible to alteration. Crozaz and Wadhwa (2001) support this contention and argue that Sr abundances measured in maskelynite by ion microprobe have not been disturbed by weathering. It is therefore likely that the initial  $^{87}\text{Sr}/^{86}\text{Sr}$  ratio of DaG estimated from the maskelynite mineral fraction is near the actual value. The relatively low initial  $^{87}\text{Sr}/^{86}\text{Sr}$  ratio of DaG is consistent with the high initial  $\epsilon_{\text{Nd}}^{143}$  value, requiring this meteorite to be derived from an incompatible-element-depleted source.

## 5. TIMING OF PLANETARY DIFFERENTIATION

The timing of planetary differentiation is most precisely defined by short-lived chronometers with half-lives less than

~100 Ma. These provide the relative time at which parent/daughter nuclides were fractionated from an initially chondritic source region. To obtain an age, however, the parent/daughter ratio of the source after differentiation must be assumed. One of the most powerful aspects of the Sm-Nd isotopic system is the fact that it is comprised of both a long-lived chronometer ( $^{147}\text{Sm} \rightarrow ^{143}\text{Nd}$ ;  $t_{1/2} = 106$  Ga) and a short-lived chronometer ( $^{146}\text{Sm} \rightarrow ^{142}\text{Nd}$ ;  $t_{1/2} = 103$  Ma). These chronometers can be used in conjunction to uniquely define the time of source formation for individual meteorites that is not dependent on an assumption about the  $^{147}\text{Sm}/^{144}\text{Nd}$  ratio of the source region after differentiation. This stems from the fact that both the age and the  $^{147}\text{Sm}/^{144}\text{Nd}$  ratio of the source can be solved for using independent decay equations for each isotopic system. To apply the dual chronometer technique the meteorite must be derived from a source that has had a relatively simple two-stage evolutionary history. The first stage corresponds to the time between planet formation and source differentiation, the second stage corresponds to the time between source formation and the partial melting event that produced the sample. Evidence for a two stage evolutionary history for the martian meteorites comes from the fact that they define a ~4.5 Ga Rb-Sr whole rock isochron (e.g., Shih et al., 1982; Jagoutz, 1991; Borg et al., 1997b). This is further supported by Pb-Pb isotopic systematics of Shergotty, Zagami, EET79001A (EETA), and Y793605 (Y79) in which the upper intercept intersects concordia at ~4.5 Ga (Chen and Wasserburg, 1986; Misawa et al., 1997).

Previously determined ages for martian silicate differentiation have been based on  $\epsilon_{\text{Nd}}^{142}$  values of nakhlites and Chassigny (NC) by Harper et al. (1995) and on  $\epsilon_{\text{Nd}}^{142} - \epsilon_{\text{Nd}}^{143}$  values of QUE (Borg et al., 1997b). Harper et al. (1995) determined an age range of 4.46–4.57 Ga, but were not able to place tighter constraints on the age because the NC source appears to have had a multi-stage history (see below). The age determined previously for martian differentiation using the two chronometer approach was 33 Ma (i.e., 4.525 Ga relative to the 4.558 Ga Pb-Pb age of the angrite LEW86010; Lugmair and Galer, 1992) and was based on the analysis of QUE by Borg et al. (1997b). Model ages determined on single samples suffer from: (1) large uncertainties because they are based on a single data point, (2) the inability to use samples with near chondritic  $\epsilon_{\text{Nd}}^{142}$  values to constrain the age of differentiation because of the large analytical uncertainties associated with  $\epsilon_{\text{Nd}}^{142}$  measurements, and (3) the required assumption that Mars initially had chondritic Sm-Nd systematics. This assumption has been called into question in the case of the Moon (Shih et al., 1993) and may not be valid for Mars given the extreme LREE/HREE fractionations observed in the meteorites (e.g., McSween, 1994).

An isochron approach to dating source differentiation using the Sm-Nd isotopic system is presented in Figure 5. Model isochrons are produced by plotting the initial  $\epsilon_{\text{Nd}}^{143}$  values of the meteorites against their present-day  $\epsilon_{\text{Nd}}^{142}$  values. For comparison, the initial  $\epsilon_{\text{Nd}}^{143}$  values of meteorites DaG, QUE, and NC are recalculated to 175 Ma, the average age of the other shergottites such as Shergotty, Zagami, Los Angeles 1, EETA/B, ALH77005 (ALH), LEW88516 (LEW), and Y793605. The model isochrons represent the age of parent/daughter fractionation (i.e., differentiation), in the source region. The present-day  $\epsilon_{\text{Nd}}^{142}$  values, as well as initial  $\epsilon_{\text{Nd}}^{143}$  values, for the martian meteorites are from whole rock and isochron measurements by

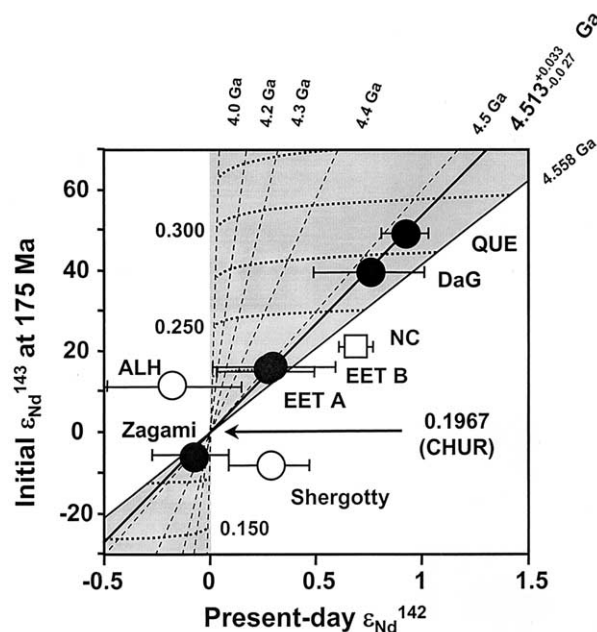


Fig. 5. Two-stage Nd isotope evolution model for the martian meteorites. Shaded area represents compositions that are consistent with a two-stage evolutionary history in which an initially chondritic source evolves (stage 1) and then undergoes differentiation (stage 2). Dashed straight lines are calculated isochrons. Dashed (near horizontal) lines represent constant  $^{147}\text{Sm}/^{144}\text{Nd}$  ratios of the source regions. Circles are shergottites and the square is the average of nakhlites and Chassigny (NC). Filled symbols are used to define the age of source formation. An age (solid isochron) of  $4.513_{-0.027}^{+0.033}$  Ga is defined by Zagami, EET79001A (EETA), EET79001B (EETB), Dar al Gani 476 (DaG), and QUE94201 (QUE). The fact that NC lies out of the two-stage evolutionary field indicated that they have had a more complex evolutionary history. Data from Wooden et al. (1982), Harper et al. (1995), Jagoutz (1996), Borg et al., 1997b, 2002, this study), Nyquist et al. (2001a,b), Shih et al. (1998, 1999), Brandon et al. (2000).

Wooden et al. (1982), Harper et al. (1995), Jagoutz (1996; unpublished data reported in Brandon et al., 2000), Borg et al., (1997b, 2002; this study), Nyquist et al. (2001a), and Shih et al. (1998, 1999). Samples that lie in the shaded field on Figure 5 have isotopic systematics that are consistent with a two-stage isotopic evolution. Samples that lie significantly above the chondritic point have Nd isotopic compositions that are consistent with derivation from LREE-depleted reservoirs, whereas samples that lie below the chondritic point have Nd isotopic compositions that are consistent with derivation from LREE-enriched reservoirs. The  $^{147}\text{Sm}/^{144}\text{Nd}$  ratios of the sources intersect the isochrons so that both the age and the  $^{147}\text{Sm}/^{144}\text{Nd}$  ratio of the source can be derived from this plot. Mixing relations are linear on this plot so that meteorites derived from a mixture of contemporaneous sources with variable  $^{147}\text{Sm}/^{144}\text{Nd}$  ratios will define an age of differentiation. This is important because it has been argued that the isotopic systematics of the martian meteorites reflect mixing of magmas derived from ~4.5 Ga depleted and enriched sources (e.g., Shih et al., 1982; Jones, 1989; Jagoutz, 1991; Borg et al., 1997b, 2002). Thus, recent mixing with, or assimilation of, an ancient evolved component will not cause individual points to deviate from the isochron, but instead will dictate their position along the iso-

chron. Therefore, although the array of data on Figure 5 most likely reflects mixing processes, the slope reflects the age of source formation.

Despite large uncertainties associated with the  $\epsilon_{\text{Nd}}^{142}$  values, the Nd isotope systematics of most shergottites form a linear array on Figure 5. Solution of the decay equations for the  $^{146}\text{Sm}$ - $^{142}\text{Nd}$  and  $^{147}\text{Sm}$ - $^{143}\text{Nd}$  chronometers demonstrate that the slope of the line regressed through the QUE, DaG, EETA, EETB, and Zagami data points corresponds to an age of  $45_{-27}^{+33}$  Ma (i.e.,  $4.513_{-0.027}^{+0.033}$  Ga relative to the 4.558 Ga Pb-Pb age of the angrite LEW86010; Lugmair and Galer, 1992). The uncertainty in the age represents the 95% confidence level as calculated following York (1966). The low value for the uncertainty underscores the fact that the  $\epsilon_{\text{Nd}}^{142}$ - $\epsilon_{\text{Nd}}^{143}$  values of the samples lie very near a single line on Figure 5. The MSWD of the regression is 0.1, reflecting large uncertainties in the  $\epsilon_{\text{Nd}}^{142}$  values. The isochron has a y-intercept of  $\epsilon_{\text{Nd}}^{143} = +0.5 \pm 1.7$  (1 sigma), indicating that it passes through the value for CHUR (chondritic uniform reservoir) and suggests that bulk Mars has chondritic Sm-Nd isotopic systematics.

Although many of the martian meteorites fall along an individual isochron on Figure 5, several meteorites do not. Shergotty, ALH77005 (ALH), and NC all lie off the two-stage model isochrons suggesting that these meteorites may have had a more complicated history. Note, however, the large analytical uncertainty associated with the  $\epsilon_{\text{Nd}}^{142}$  measurement for ALH, which permits the ALH source to be derived by a two-stage growth between 0 and 4.49 Ga. In contrast to ALH, Shergotty and NC lie to the right of the 4.558 Ga isochron. Differences between the isotopic systematics of Shergotty and Zagami suggest that the Shergotty  $\epsilon_{\text{Nd}}^{142}$  analysis could be in error. The NC point, however, is the weighted average of analyses of three different nakhlites, as well as Chassigny. It therefore seems likely that the sources of NC (and Shergotty) must have undergone multiple stages of evolution.

The Sm-Nd isotopic systematics of the nakhlites are problematic because they indicate that these meteorites are derived from LREE-depleted sources, whereas their bulk rock REE patterns indicate derivation from LREE-enriched sources. This has generally been attributed to formation of the nakhlites by small degrees of partial melting (e.g., Longhi, 1991; Borg et al., 1997b; Shih et al., 1999). In this scenario, however, the nakhlites would fall on a two stage model isochron in Figure 5. The fact that they do not, suggests instead, that their source region has been modified through the addition of a LREE-enriched component. The composition of the LREE-enriched component present in the NC source can be constrained with binary mixing calculations. The mixing event is modeled at 1.3 Ga, the age of the nakhlites and Chassigny. The depleted mantle source is assumed to have the Sm-Nd isotopic systematics of the QUE source at 1.3 Ga (Fig. 6a) and thus have  $^{147}\text{Sm}/^{144}\text{Nd} = 0.285$ ,  $\epsilon_{\text{Nd}}^{143} = +35$ , and  $\epsilon_{\text{Nd}}^{142} = +0.92$ . The results of the calculations are dependent on the  $^{147}\text{Sm}/^{144}\text{Nd}$  ratio that the LREE-enriched component is assumed to have. For example, if the LREE-enriched component has a  $^{147}\text{Sm}/^{144}\text{Nd}$  ratio of 0.09, then it must also have a  $\epsilon_{\text{Nd}}^{143} = +7$  and an  $\epsilon_{\text{Nd}}^{142} = +0.58$ , whereas if it has a  $^{147}\text{Sm}/^{144}\text{Nd}$  ratio of 0.13, then it must have a  $\epsilon_{\text{Nd}}^{143} = +12$  and an  $\epsilon_{\text{Nd}}^{142} = +0.64$ . The  $\epsilon_{\text{Nd}}^{142}$  and  $\epsilon_{\text{Nd}}^{143}$  values of the LREE-enriched component must be more positive if the enrichment event occurred before 1.3 Ga. Thus, in all cases the  $\epsilon_{\text{Nd}}$  values of the LREE-enriched com-

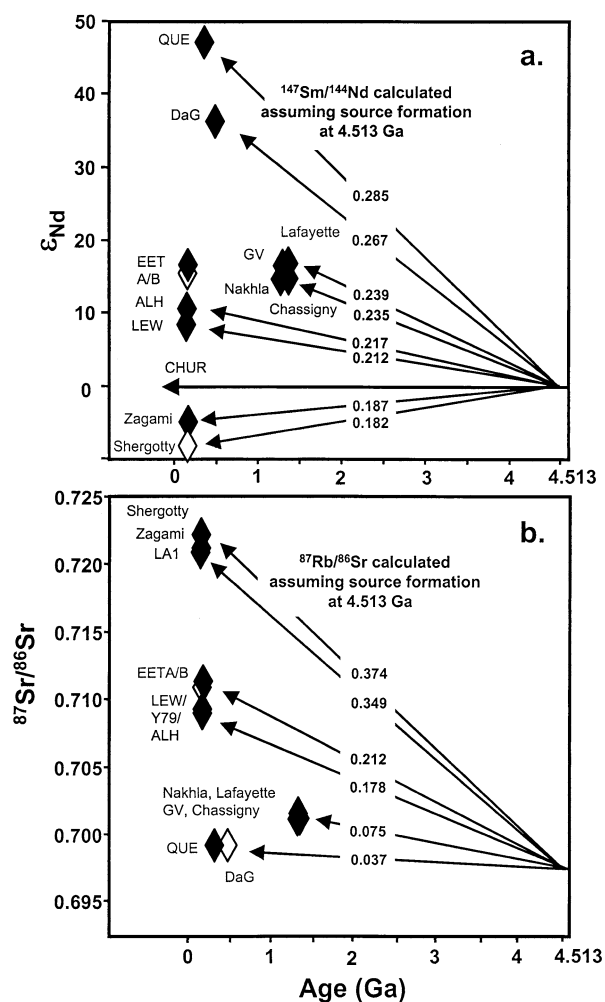


Fig. 6. Age (T) versus initial Nd and Sr isotopic compositions (I) diagrams. Ages are preferred ages of Nyquist et al. (2001b) and initial isotopic compositions of the martian meteorites were determined by Nyquist et al. (1979, 1995, 2000, 2001a), Wooden et al. (1982), Jagoutz (1996), Borg et al. (1997b, 2002), Shih et al. (1998, 1999), Morikawa et al. (2001). The initial isotopic compositions of meteorites plotted with solid diamonds are determined from their internal isochrons, whereas the initial isotopic compositions of meteorites plotted with open diamonds are calculated from their whole rock isotopic compositions and either their Rb-Sr or Sm-Nd ages. (a) Plot of age versus initial  $\epsilon_{\text{Nd}}$  values. The  $^{147}\text{Sm}/^{144}\text{Nd}$  ratios are calculated for the source regions assuming differentiation from a chondritic reservoir at 4.513 Ga and range from 0.182 (Shergotty) to 0.285 (QUE94201). (b) Plot of age versus initial  $^{87}\text{Sr}/^{86}\text{Sr}$  ratio. The  $^{87}\text{Rb}/^{86}\text{Sr}$  ratios are calculated for the source regions assuming differentiation from a reservoir with the composition estimated for bulk Mars ( $^{87}\text{Rb}/^{86}\text{Sr} = 0.16$ ) at 4.513 Ga and range from 0.374 (Shergotty) to 0.037 (QUE).

ponent are required to be positive, requiring this component to be derived from an ancient LREE-depleted source. A possible origin of this component is incompatible-element-enriched fluids or melts derived from a depleted mantle source.

## 6. PARENT/DAUGHTER RATIOS OF MARTIAN METEORITE SOURCES

Both short and long-lived isotopic systems demonstrate evidence for a differentiation event early in martian history. This

Table 3. Parent/daughter ratios of martian meteorite sources.<sup>a</sup>

	Age (Ma)	Mg# parent	La/Yb	<sup>87</sup> Rb/ <sup>86</sup> Sr	<sup>147</sup> Sm/ <sup>144</sup> Nd	<sup>176</sup> Lu/ <sup>177</sup> Hf	<sup>187</sup> Re/ <sup>188</sup> Os	<sup>180</sup> Hf/ <sup>183</sup> W
Shergotty	165	32	1.26	0.374	0.182	0.0279		134
Zagami	177		1.16	0.357	0.187	0.0276	0.512	144
LA1	170		1.40	0.349	0.186			
EET79001A	173	54	0.33	0.209	0.224	0.0444	0.390	244
EET79001B	173		0.37	0.215	0.226	0.0441	0.394	
ALH77005	179	71	0.58	0.183	0.217	0.0439	0.477	134
LEW88516	178	61	0.51	0.178	0.212		0.475	
Y793605	172		0.50	0.180			0.456	
DaG476 <sup>1</sup>	474		0.15	0.037	0.267		0.420	
DaG476 <sup>2</sup>	474						0.533	
QUE94201	327	38	0.11	0.037	0.285	0.0482		
Nakhla	1270	26–44	6.37	0.074	0.236		1.148	290
Governador Valadares	1330		5.54	0.072	0.239			
Lafayette	1320		4.89	0.077	0.238		0.371	
Chassigny	1340	41	4.92	0.076	0.236		0.296	240

<sup>a</sup> Parent/daughter ratios of meteorite source regions are calculated from initial Sr, Nd, Hf, and Os isotopic compositions, and whole rock  $\epsilon_w^{182}$  values assuming differentiation at 4.513 Ga. Initial Sr and Nd isotopic compositions are determined from mineral isochrons except for EETB (Nd) and DaG (Sr). Initial Hf and Os are calculated from whole rock isotopic compositions using preferred ages of Nyquist et al. (2001b) and the Y793605 age of Morikawa et al. (2001). Two <sup>187</sup>Re/<sup>188</sup>Os ratios are calculated for DaG using data from (1) Brandon et al. (2000) and (2) Walker et al. (2002). The calculations assume that undifferentiated source regions had chondritic Sm-Nd, Lu-Hf, Re-Os, and Hf-W isotopic systematics and Rb-Sr isotopic systematics estimated for bulk Mars (see text). Decay constants used in modeling are:  $\lambda(^{87}\text{Rb}) = 0.01402 \text{ (Ga)}^{-1}$ ;  $\lambda(^{147}\text{Sm}) = 0.00654 \text{ (Ga)}^{-1}$ ;  $\lambda(^{176}\text{Lu}) = 0.0193 \text{ (Ga)}^{-1}$ ;  $\lambda(^{187}\text{Re}) = 0.01666 \text{ (Ga)}^{-1}$ ;  $\lambda(^{182}\text{Hf}) = 0.077 \text{ (Ma)}^{-1}$ . Data from Blichert-Toft et al. (1999); Borget et al. (1997b, 2002, this study); Brandon et al. (2000); Jagoutz (1996); Lee and Halliday (1997); Morikawa et al. (2001); Nakamura et al. (1982a,b); Nyquist et al. (1979, 1995, 2000, 2001a); Papanastassiou and Wasserburg (1974); Shih et al. (1998, 1999); Walker et al. (2002); Wooden et al. (1979, 1982). Parent magma Mg# from Stolper and McSween (1979), Treiman (1986), McSween et al. (1988, 1996), Longhi and Pan (1989), Harvey et al. (1993). La/Yb whole rock data from Schmitt and Smith (1963), Shih et al. (1982), Nakamura et al. (1982a,b), Burghelle et al. (1983), Dreibus et al. (1992), Mittlefehldt et al. (1997), Rubin et al. (2000), and Zipfel et al. (2000).

is evident in the Rb-Sr isotopic system by the fact that the meteorites define a 4.5 Ga whole rock isochron (e.g., Shih et al., 1982; Jagoutz, 1991; Borg et al., 1997b) and in the Sm-Nd isotopic system by the two-stage model Nd isochron age of ~4.51 Ga (Fig. 5). That these isotopic systematics are preserved in relatively young rocks indicates that their source regions have not been significantly modified by geochemical processes since they formed (e.g., Borg et al., 1997b). It also indicates that the isotopic compositions of the meteorites directly reflect the composition of their sources at the time of source formation. As a result, the isotopic compositions of the meteorites can be used to constrain the long-term parent/daughter ratios of their sources.

### 6.1. Sm-Nd and Rb-Sr Isotopic Systematics

Figure 6a is a Time versus Initial (T-I)  $\epsilon_{\text{Nd}}$  diagram in which the ages of martian meteorites determined from their Sm-Nd isochrons are plotted against their initial  $\epsilon_{\text{Nd}}^{143}$  values. In cases where only Rb-Sr data is available, the initial Nd isotopic composition is estimated using the whole rock composition and the age of the meteorite (open symbols). Growth curves depicting time averaged <sup>147</sup>Sm/<sup>144</sup>Nd ratios of the source regions have been calculated assuming the sources formed at 4.513 Ga. The first stage of isotopic evolution occurs in an undifferentiated (chondritic) reservoir, whereas the second stage of growth occurs in a differentiated reservoir.

The calculated <sup>147</sup>Sm/<sup>144</sup>Nd ratios in Figure 6a are the same as those plotted on the  $45_{-27}^{+33}$  model isochron diagram (Fig. 5) and are presented along with other source region parent/daughter ratios in Table 3. It is apparent from Figures 5 and 6a that

the source regions for the martian meteorites display a large range of time-averaged <sup>147</sup>Sm/<sup>144</sup>Nd ratios, consistent with ~55 epsilon units of variation of initial  $\epsilon_{\text{Nd}}^{143}$  values. The Shergotty source is the most LREE-enriched and is calculated to have a <sup>147</sup>Sm/<sup>144</sup>Nd ratio of 0.182, whereas the QUE source is the most LREE-depleted and has a <sup>147</sup>Sm/<sup>144</sup>Nd ratio of 0.285. Only a few of the meteorites analyzed fall on the same growth curve in Figure 6a, indicating that they could be derived from the same source. Examples of these include the nakhlites and Chassigny, as well as EETA and EETB. All of the other meteorites have initial  $\epsilon_{\text{Nd}}^{143}$  values that differ enough to preclude them from being derived from the same source regions. The DaG source region is similar to the QUE source region, having a <sup>147</sup>Sm/<sup>144</sup>Nd ratio of 0.267, but is not as LREE-depleted. Thus, although DaG and QUE have similar REE patterns, they must be derived from distinct source regions. Furthermore, despite having a more mafic parental melt composition, DaG appears to be derived from a less incompatible-element-depleted source region than QUE.

The first stage of Sr isotopic growth in an undifferentiated martian meteorite reservoir cannot be modeled without an estimate of the bulk <sup>87</sup>Rb/<sup>86</sup>Sr ratio of the planet. However, variations in volatile element abundances in the terrestrial planets prevents chondritic <sup>87</sup>Rb/<sup>86</sup>Sr ratios from representing bulk Mars. Borg et al. (1997b) estimated the <sup>87</sup>Rb/<sup>86</sup>Sr ratio of bulk Mars to be 0.16 by dividing the martian Rb/Ca ratio by the terrestrial Sr/Ca ratio determined by Jagoutz et al. (1979), Wänke and Dreibus (1988), and Longhi et al. (1992). This approach assumes that martian and terrestrial Sr/Ca ratio is the same. This value is slightly higher than the value of 0.13

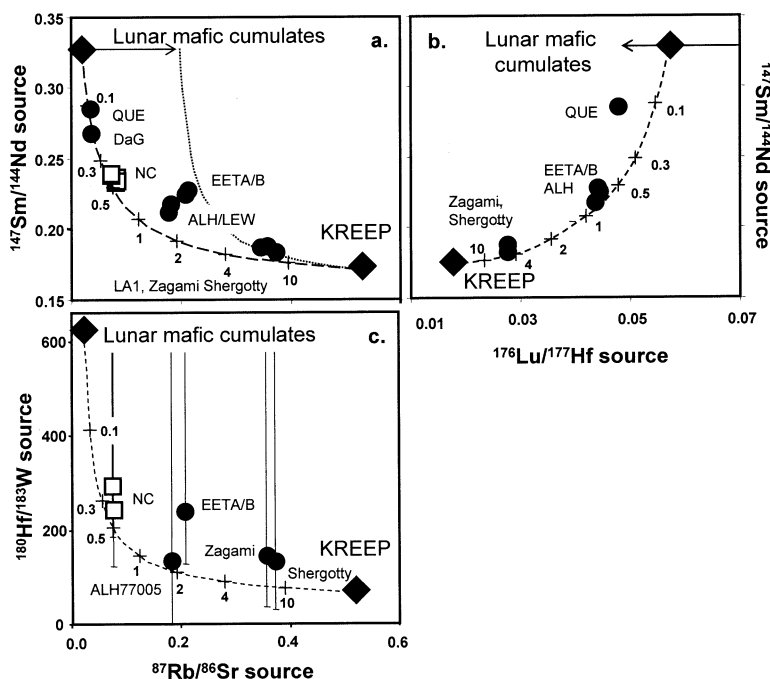


Fig. 7. Plots of parent/daughter ratios calculated for martian meteorite sources. Symbols same as Figure 5. Diamonds represent lunar sources. (a, b) Plots of  $^{87}\text{Rb}/^{86}\text{Sr}$  versus  $^{147}\text{Sm}/^{144}\text{Nd}$  and  $^{147}\text{Sm}/^{144}\text{Nd}$  versus  $^{176}\text{Lu}/^{177}\text{Hf}$  ratios calculated for the martian meteorite source regions. Parent/daughter isotope ratios of sources are calculated from the initial Sr, Nd, and Hf isotopic compositions of the martian meteorites (data same as Fig. 7; Blichert-Toft et al., 1999) assuming derivation by two stage evolution (see Fig. 7 and Table 3). Mafic lunar mantle source compositions estimated by Snyder et al. (1992, 1994) are plotted along with the values for KREEP estimated by Warren and Wasson (1979). Horizontal arrows represent range of values postulated for lunar cumulates (see text). These compositions are used as end-members of mixing models (coarse dashed lines). The depleted lunar mantle source is estimated by Snyder et al. (1992) to have Rb = 0.05 ppm, Sr = 7.8 ppm,  $^{87}\text{Rb}/^{86}\text{Sr}$  = 0.018, Sm = 0.27 ppm, Nd = 0.52 ppm,  $^{147}\text{Sm}/^{144}\text{Nd}$  = 0.328, Lu = 0.24 ppm, Hf = 0.58 ppm, and  $^{176}\text{Lu}/^{177}\text{Hf}$  = 0.057. KREEP is estimated by Warren and Wasson (1979) to have Rb = 37 ppm, Sr = 200 ppm,  $^{87}\text{Rb}/^{86}\text{Sr}$  = 0.52, Sm = 49 ppm, Nd = 180 ppm,  $^{147}\text{Sm}/^{144}\text{Nd}$  = 0.172, Lu = 5 ppm, Hf = 38 ppm, and  $^{176}\text{Lu}/^{177}\text{Hf}$  = 0.018. Fine dashed line in Figure 8a is a mixing line between KREEP and the mafic cumulate with a 10 times greater Rb abundance (Rb = 0.5). Note that the isotopic variability of the martian meteorite source regions is consistent with mixing between these end-members. Note that a better fit of the shergottite data on Figure 7b would be attained if the lower  $^{176}\text{Lu}/^{177}\text{Hf}$  ratios calculated for depleted mantle sources by Beard et al. (1998) are used in the place of the values estimated by Snyder et al. (1992). (c) Plot of  $^{87}\text{Rb}/^{86}\text{Sr}$  versus  $^{180}\text{Hf}/^{183}\text{W}$  ratios calculated for the martian meteorite source regions. The  $^{180}\text{Hf}/^{183}\text{W}$  ratios of sources are calculated from the present-day  $\epsilon_{\text{W}}^{182}$  values of the martian meteorites (Lee and Halliday, 1997) assuming derivation by two stage evolution (see text). Correlation between  $^{87}\text{Rb}/^{86}\text{Sr}$  and  $^{180}\text{Hf}/^{183}\text{W}$  ratios of martian meteorite sources suggest that Hf and W were fractionated in the silicate portion of Mars when  $^{182}\text{Hf}$  was still actively decaying. The  $^{180}\text{Hf}/^{183}\text{W}$  ratio of the mafic lunar mantle source is estimated to be the same as low-Ti mare basalt 15545 and 15546 ( $^{180}\text{Hf}/^{183}\text{W}$  = 618) analyzed by Neal (2001) and have the same Hf abundance as modeled in Figure 7b (Snyder et al., 1992). The  $^{180}\text{Hf}/^{183}\text{W}$  ratio and Hf and W abundances for KREEP ratio is from Warren and Wasson (1979). The mixing model (coarse dashed line) is able to reproduce most of the martian meteorite source compositions, but unable to reproduce the  $^{180}\text{Hf}/^{183}\text{W}$  ratios of the EET79001A/B sources. Like the models presented in Figures 7a,b, EET79001A/B lies above the mixing line in this figure suggesting that it is derived from a mafic cumulate source region that has a higher Rb/Sr ratio than the cumulates sources of the other shergottites.

calculated by Shih et al. (1999) using K/La ratios of the martian meteorites. However, the  $^{87}\text{Rb}/^{86}\text{Sr}$  ratios calculated for the sources, assuming source formation at 4.513 Ga are not strongly affected by the  $^{87}\text{Rb}/^{86}\text{Sr}$  ratio assumed for bulk Mars. This stems from the fact, that there is a very limited amount of time ( $\sim 45$  Ma) for bulk Mars to evolve before planetary differentiation and source formation. For example, the  $^{87}\text{Rb}/^{86}\text{Sr}$  ratios calculated for the meteorite source regions are changed by  $<0.6\%$  if bulk Mars had a  $^{87}\text{Rb}/^{86}\text{Sr}$  ratio 0.5 instead of 0.16. The  $^{87}\text{Rb}/^{86}\text{Sr}$  ratios of the sources, presented in Table 3 and Figure 6a and used throughout the manuscript, are calculated assuming source formation at 4.513 Ga using a  $^{87}\text{Rb}/^{86}\text{Sr}$  ratio of bulk Mars of 0.16.

The meteorite sources display a very large range of  $^{87}\text{Rb}/^{86}\text{Sr}$  ratios that correlate inversely with the  $^{147}\text{Sm}/^{144}\text{Nd}$  ratios calculated for the meteorite sources (Fig. 7a). The most depleted martian sources have a  $^{87}\text{Rb}/^{86}\text{Sr}$  ratio near 0.04, whereas the most enriched sources have a  $^{87}\text{Rb}/^{86}\text{Sr}$  ratio of 0.37. Figure 6b demonstrates that DaG and QUE appear to lie on a single growth curve, consistent with derivation from a single source. The  $^{147}\text{Sm}/^{144}\text{Nd}$  ratios calculated for their source regions, however, differ outside analytical uncertainty. This inconsistency is typical of the martian meteorites. For example, the ilherzolithic shergottites ALH and LEW have very similar initial Sr isotopic compositions and therefore are derived from Lu sources with similar  $^{87}\text{Rb}/^{86}\text{Sr}$  ratios, whereas their

initial  $\epsilon_{\text{Nd}}^{143}$  values differ by  $\sim 3$  epsilon units and fall on different growth curves (Figs. 6a,b). Ultimately, this must reflect a greater fractionation of  $^{147}\text{Sm}/^{144}\text{Nd}$  ratios in the sources compared to the  $^{87}\text{Rb}/^{86}\text{Sr}$  ratios.

The range of  $^{147}\text{Sm}/^{144}\text{Nd}$  and  $^{87}\text{Rb}/^{86}\text{Sr}$  ratios calculated for the martian sources are similar to source regions estimated for the Moon. For example, the range of  $^{147}\text{Sm}/^{144}\text{Nd}$  ratio estimated for the source region for KREEP basalts and various Mg-suite rocks is 0.169–0.175 (Shih et al., 1992; Snyder et al., 1992, 1994) and is similar to the ratio of 0.18 estimated for the Shergotty source. The range of  $^{147}\text{Sm}/^{144}\text{Nd}$  ratios estimated for depleted mare basalt sources is 0.26–0.33 (e.g., Unruh et al., 1984) and is similar to the ratio estimated for the DaG and QUE source region of 0.27–0.29. These similarities suggest that the sources of the martian meteorites and lunar samples may have undergone a similar amount of Sm-Nd fractionation. The  $^{87}\text{Rb}/^{86}\text{Sr}$  ratios for the martian and lunar sources are not directly comparable because the Moon is thought to have lower volatile element abundances than Mars (e.g., Dreibus and Wänke, 1985). However, if the calculated  $^{87}\text{Rb}/^{86}\text{Sr}$  ratios of the sources are adjusted for planetary differences in Rb ( $\sim$ two-fold increase; see above), similarities between some of the ratios become clearer. For example, the  $^{87}\text{Rb}/^{86}\text{Sr}$  ratio for KREEP has been estimated to be 0.23 (Warren and Wasson, 1979; Snyder et al., 1994) and is lower than the value of 0.37 estimated for the Shergotty source by a factor of  $\sim 1.6$  (Fig. 6b). However, the depleted lunar mantle is estimated to have a  $^{87}\text{Rb}/^{86}\text{Sr}$  ratio of 0.002–0.009 (e.g., Nyquist, 1977; Paces et al., 1991; Nyquist and Shih, 1992) and is below the value estimated for the QUE source region of 0.036. Increasing the Rb abundance in the depleted lunar mantle component in proportion to the estimated differences in bulk Rb abundance in Moon and Mars yields a source that still has a  $^{87}\text{Rb}/^{86}\text{Sr}$  ratio that is lower than the ratio estimated for the QUE source region.

## 6.2. Lu-Hf Isotopic Systematics

The  $^{176}\text{Lu}/^{177}\text{Hf}$  ratios for the martian meteorite sources have been calculated from the present-day whole rock  $^{176}\text{Lu}/^{177}\text{Hf}$  and  $^{176}\text{Hf}/^{177}\text{Hf}$  ratios determined by Blichert-Toft et al. (1999) using the preferred isochron ages of Nyquist et al. (2001b), assuming differentiation from a chondritic source ( $\text{CHUR}(0) = ^{176}\text{Hf}/^{177}\text{Hf} = 0.282772$ ;  $^{176}\text{Lu}/^{177}\text{Hf} = 0.0332$ ; Blichert-Toft and Albarède, 1997) at 4.513 Ga (Table 3). Although the Hf isotope data set is limited, it does include shergottites that exhibit the entire range of REE patterns and initial Sr and Nd isotopic compositions. The calculated  $^{176}\text{Lu}/^{177}\text{Hf}$  ratios correlate well with  $^{147}\text{Sm}/^{144}\text{Nd}$  and  $^{87}\text{Rb}/^{86}\text{Sr}$  ratios calculated for the meteorite sources (Fig. 7b; Table 3). The  $^{176}\text{Lu}/^{177}\text{Hf}$  ratios calculated for the sources of QUE, EETA/B, ALH, Zagami, and Shergotty range from 0.028 to 0.048. Like the  $^{87}\text{Rb}/^{86}\text{Sr}$  and  $^{147}\text{Sm}/^{144}\text{Nd}$  ratios calculated for the martian meteorite sources, the  $^{176}\text{Lu}/^{177}\text{Hf}$  ratios are similar to ratios estimated for some lunar basalt sources. For example, the range of  $^{176}\text{Lu}/^{177}\text{Hf}$  ratios for sources of lunar low-Ti basalts calculated from the Hf isotopic data of Unruh et al. (1984), assuming lunar cumulate formation at 4.50 Ga, is 0.048–0.049. Although these values are typical of mare basalt source regions, a few lunar basalts, such as the Apollo 12 ilmenite basalts, are estimated to have significantly higher

$^{176}\text{Lu}/^{177}\text{Hf}$  ratios (0.078–0.084) than the martian meteorite sources. Despite the fact that KREEP-rich lunar basalts have not been analyzed, Snyder et al. (1992) and Warren and Wasson (1979) estimated the KREEP source (ur-KREEP) to have a  $^{176}\text{Lu}/^{177}\text{Hf}$  ratio of 0.015 to 0.018, which is similar, but slightly lower than the Shergotty source. Thus, martian and lunar basalt sources appear to have similar ranges and values for  $^{176}\text{Lu}/^{177}\text{Hf}$ , as well as  $^{87}\text{Rb}/^{86}\text{Sr}$  and  $^{147}\text{Sm}/^{144}\text{Nd}$  ratios.

## 6.3. Hf-W Isotopic Systematics

The  $^{180}\text{Hf}/^{183}\text{W}$  ratio of martian sources is constrained by the short-lived isotopic system  $^{182}\text{Hf} \rightarrow ^{182}\text{W}$  ( $t_{1/2} = 9$  Ma). All of the martian meteorites have positive  $\epsilon_{\text{W}}^{182}$  values relative to both terrestrial and recently reported chondritic W isotopic compositions (Lee and Halliday, 1997; Ireland et al., 2000; Kleine et al., 2002; Yin et al., 2002) and are interpreted to reflect high  $^{182}\text{Hf}/^{183}\text{W}$  ratios in silicate Mars as a result of core formation (Lee and Halliday, 1997). To maintain consistent notation,  $\epsilon_{\text{W}}^{182}$  values are calculated relative to chondritic W isotopic compositions reported by Kleine et al. (2002) and not terrestrial W isotopic compositions (Lee and Halliday, 1997). The difference is +1.9 epsilon units. The samples analyzed so far have recalculated  $\epsilon_{\text{W}}^{182}$  values from +2.2 to +4.9, too broad a range to be caused solely by core-mantle differentiation (Snyder et al., 2000; Halliday et al., 2001). The  $^{180}\text{Hf}/^{183}\text{W}$  ratios of the martian meteorite sources are calculated using the  $\epsilon_{\text{W}}^{182}$  values of Lee and Halliday (1997) normalized to the chondritic W isotopic compositions determined by Kleine et al. (2002), eqn. 3 from Harper and Jacobson (1996), and the  $45_{-27}^{+33}$  Ma age from Figure 5. The chondritic atomic Hf/W ratio used in the calculation is 1.16 (Anders and Grevesse, 1989; Palme and Beer, 1993) and the solar system initial  $^{182}\text{Hf}/^{180}\text{Hf}$  ratio is  $1 \times 10^{-4}$  (Ireland et al., 2000; Kleine et al., 2002; Yin et al., 2002).

The  $^{180}\text{Hf}/^{183}\text{W}$  ratios calculated for the martian meteorite source regions vary from 134 for Shergotty to 290 for Nakhla, but are highly dependent on the assumed age of source formation. Thus, the uncertainty in the calculated  $^{180}\text{Hf}/^{183}\text{W}$  ratios is +90% and –650% at the 2-sigma confidence level of the Nd model age. Furthermore, the  $^{180}\text{Hf}/^{183}\text{W}$  ratios calculated for the martian meteorite source regions are also dependent on the solar system initial  $^{182}\text{Hf}/^{180}\text{Hf}$  ratio and the  $\epsilon_{\text{W}}^{182}$  value of chondrites used in the calculations, and these values are not well established. For example, if the  $^{182}\text{Hf}/^{180}\text{Hf}$  ratio used in the calculation is  $2 \times 10^{-5}$  (Harper and Jacobson, 1996), and the  $\epsilon_{\text{W}}^{182}$  values of the meteorites are calculated by normalizing to terrestrial standards (e.g., Lee and Halliday, 1997), the  $^{180}\text{Hf}/^{183}\text{W}$  ratio calculated for the martian meteorite sources range from 100 to 880.

Despite these uncertainties, the  $^{180}\text{Hf}/^{183}\text{W}$  ratios calculated for the martian meteorite sources exhibit a range of values that correlate with the  $^{87}\text{Rb}/^{86}\text{Sr}$ ,  $^{147}\text{Sm}/^{144}\text{Nd}$ , and  $^{176}\text{Lu}/^{177}\text{Hf}$  ratios calculated for the meteorite sources (Fig. 7c, Table 3). It therefore seems likely that the sources of the martian meteorites have a range of  $^{180}\text{Hf}/^{183}\text{W}$  ratios, and that this range was produced by the same process that fractionated Rb/Sr, Sm/Nd, and Lu/Hf ratios in the martian meteorite sources. The  $^{180}\text{Hf}/^{183}\text{W}$  ratio of the Shergotty source region ( $\sim 134$ ) is similar to that estimated for KREEP of 39–65 (Warren and Wasson,

1979). Likewise, some Apollo 15 low Ti basalts have  $^{180}\text{Hf}/^{183}\text{W}$  ratios as high as  $\sim 700$  (Neal, 2001), suggesting that depleted lunar mantle could have  $^{180}\text{Hf}/^{183}\text{W}$  ratios similar to the values of some of the martian meteorites. The fact that the martian meteorite sources have parent/daughter ratios that are similar to lunar sources produced by crystallization from a magma ocean suggests that the variability of  $^{180}\text{Hf}/^{183}\text{W}$  ratios observed in the martian meteorite sources could result from fractionation of W from Hf during crystallization of a magma ocean.

#### 6.4. Re-Os Isotopic Systematics

The Re-Os isotopic system has also been applied to a large number of martian meteorites (Brandon et al., 2000; Walker et al., 2002). The  $^{187}\text{Re}/^{188}\text{Os}$  ratios of the meteorite sources are calculated using the preferred isochron ages of Nyquist et al. (2001b), assuming differentiation from a source at 4.513 Ga that evolved from solar system initial Re-Os values ( $^{187}\text{Re}/^{188}\text{Os} = 0.09531$ ;  $^{187}\text{Os}/^{188}\text{Os} = 0.40186$ ; Shirey and Walker, 1998). The  $^{187}\text{Re}/^{188}\text{Os}$  ratios calculated for the meteorite sources, however, do not correlate with the parent/daughter ratios determined for the other isotopic systems discussed above (Table 3). The lack of correlation between  $^{187}\text{Re}/^{188}\text{Os}$  ratios and  $^{87}\text{Rb}/^{86}\text{Sr}$ ,  $^{147}\text{Sm}/^{144}\text{Nd}$ , and  $^{176}\text{Lu}/^{177}\text{Hf}$  ratios calculated for the meteorite sources may imply that the Re-Os systematics are not affected by the mixing processes that seem to control the other isotopic systems and/or are more strongly controlled by another process, such as assimilation. Another explanation is that the  $^{187}\text{Re}/^{188}\text{Os}$  ratios calculated for the sources are strongly influenced by the initial  $^{187}\text{Os}/^{188}\text{Os}$  ratios calculated for the meteorites, and that some of these are strongly affected by corrections for in situ decay. To generate correlations between initial  $^{187}\text{Os}/^{188}\text{Os}$  ratios and other isotopic systems, Brandon et al. (2000) assumed that Nakhla had a crystallization age of 1.42 Ga and DaG had a crystallization age of 726 Ma. The apparent correlation of  $^{187}\text{Os}/^{188}\text{Os}$  ratios with  $\epsilon_{\text{Nd}}^{142}$  and  $\epsilon_{\text{W}}^{182}$  values disappears if measured internal isochron ages of 1.23–1.36 Ga for Nakhla (Papanastassiou and Wasserburg, 1974; Gale et al., 1975; Nakamura et al., 1982a) and 474 Ma for DaG are used. The  $^{187}\text{Re}/^{188}\text{Os}$  ratio of the source regions of some meteorites are also strongly dependent on the whole rock  $^{187}\text{Re}/^{188}\text{Os}$  ratio. Thus, Re mobility resulting from weathering could also affect the calculated  $^{187}\text{Re}/^{188}\text{Os}$  ratio of the sources.

### 7. GENERATION OF THE RANGE OF METEORITE SOURCE COMPOSITIONS

#### 7.1. Mixing Models

The trace element and isotopic variations observed in the martian meteorites have been attributed to both crustal differentiation and melting of compositionally distinct source regions (e.g., Shih et al., 1982; Jones, 1989; Jagoutz, 1991; Borg et al., 1997a,b, 2002; Herd et al., 2002). From a purely chemical perspective, it is difficult to tell these processes apart. However, the fact that the parent/daughter ratios that are required to produce the Sr, Nd, and Hf (and possibly W) isotopic compositions of the martian meteorites are similar to the range of parent/daughter ratios calculated for lunar cumulates and late

stage liquids suggests that much of the variability observed in the Rb-Sr, Sm-Nd, Lu-Hf, and Hf-W isotopic systematics of the martian meteorites could reflect interactions between compositionally distinct sources at the time of partial melting.

To test this hypothesis, mixing models are constructed to determine if the variation of calculated source  $^{87}\text{Rb}/^{86}\text{Sr}$ ,  $^{147}\text{Sm}/^{144}\text{Nd}$ , and  $^{176}\text{Lu}/^{177}\text{Hf}$  ratios are consistent with mixing of crystallization products of a lunar magma ocean. The composition of lunar mafic cumulates and KREEP are used to define the ends of the mixing arrays in Figures 7a,b. The compositions of the mafic cumulate end-member is from Snyder et al. (1992, 1994), whereas the composition of KREEP is that proposed by Warren and Wasson (1979). The concentration of Rb in the sources has been increased by a factor of  $\sim 2$  to account for the greater volatile element abundances on Mars relative to the Moon (e.g., Dreibus and Wänke, 1985; Wänke and Dreibus, 1988). The composition of the depleted martian component is presented in the caption of Figure 7.

The results of the mixing models are presented in Figures 7a,b. From Figure 7a it is clear that mixing of end-members with compositions similar to the most depleted and enriched lunar mantle components reproduces the  $^{87}\text{Rb}/^{86}\text{Sr}$  and  $^{147}\text{Sm}/^{144}\text{Nd}$  ratios of most of the martian meteorite sources. The nakhlites fall on the source mixing line on Figure 7a, as is expected if their isotopic systematics reflected the long-term parent/daughter ratios of their source regions. This is consistent with production of their LREE-enriched bulk rock compositions near the time of partial melting in the mantle. The variation in the  $^{176}\text{Lu}/^{177}\text{Hf}$  ratios calculated for the martian meteorites can also be reproduced by mixing lunar mantle components (Fig. 7b). Note that although there is a range in  $^{176}\text{Lu}/^{177}\text{Hf}$  ratios proposed for mafic lunar basalt sources (e.g., Beard et al., 1998), and that a better fit of the data could be obtained using a mafic cumulate end-member with a lower  $^{176}\text{Lu}/^{177}\text{Hf}$  ratio, the composition proposed by Snyder et al. (1992) is used in the models to maintain consistency with the  $^{87}\text{Rb}/^{86}\text{Sr}$ - $^{147}\text{Sm}/^{144}\text{Nd}$  mixing model (Fig. 7a). Despite this complication, the proportions of end-members required to reproduce the parent/daughter ratios of individual meteorite sources is consistent in both mixing models, suggesting that the proportions of elements used in the models are approximately correct.

The only meteorite that falls significantly above the source mixing line in Figure 7a is EETA/B, suggesting that it is derived from a source that is compositionally distinct from the sources of the other meteorites. This is consistent with isotope mixing models produced by Jones (1989) in which the lherzolitic shergottites and EETA/B plotted in reversed order on various diagrams. Jagoutz (1991) also suggested that a third source was present on Mars to account for the inconsistent behavior of EETA/B on mixing diagrams. A second mafic cumulate source region, characterized by higher  $^{87}\text{Rb}/^{86}\text{Sr}$  ratio than the depleted mafic cumulate source would satisfy the mixing relations for EETA/B (fine dashed curve Fig. 7a). The higher  $^{87}\text{Rb}/^{86}\text{Sr}$  of this source region probably reflects the presence of a phase in which Rb is slightly more compatible. This phase must sequester Rb, but have a relatively low affinity for Sr, Hf, and the REEs. One phase that satisfies these criteria, and could be present in the martian mantle, is amphibole (Borg et al., 2002; Herd et al., 2002). Thus, a mafic source containing

amphibole is expected to have similar  $^{147}\text{Sm}/^{144}\text{Nd}$  and  $^{176}\text{Lu}/^{177}\text{Hf}$  ratios as a more depleted, amphibole-free mafic cumulate source and therefore yield mixing relations that appear binary on Figure 7b.

Although there is a limited set of measured  $\epsilon_{\text{W}}^{182}$  values, and calculated  $^{180}\text{Hf}/^{183}\text{W}$  ratios of the sources have huge uncertainties associated with them, mixing models have also been constructed for the Hf-W system (Fig. 7c). The KREEP end-member is defined to have a  $^{180}\text{Hf}/^{183}\text{W}$  ratio of 45 (Warren and Wasson, 1979) and the Hf abundance discussed above. The  $^{180}\text{Hf}/^{183}\text{W}$  ratio of the mafic cumulates is defined by the average ratio observed in low-Ti mare basalts 15545 and 15546 analyzed by Neal (2001);  $^{180}\text{Hf}/^{183}\text{W} = 618$ , and the Hf abundances discussed above. Shergotty, Zagami, ALH, Nakhla, and Chassigny appear to lie near a single mixing line on Figure 7c, although EETA/B does not. Instead, EETA/B appears to lie on a mixing line between a KREEP-like component and a mantle source region characterized by higher  $^{87}\text{Rb}/^{86}\text{Sr}$  ratio, again suggesting that the source region of this meteorite contains a mafic component characterized by a relatively high  $^{87}\text{Rb}/^{86}\text{Sr}$  ratio.

The ability of the mixing models to reproduce the source compositions calculated for the martian meteorites using lunar end-members supports the idea that trace element and isotopic variability observed in the martian meteorites reflects interactions of compositionally diverse sources. Strongly depleted incompatible element sources on the Moon are thought to have been formed by crystallization and accumulation of mafic silicates from the lunar magma ocean, whereas KREEP is thought to represent highly fractionated late stage magma. If the analogy between Mars and the Moon is appropriate, Mars had a magma ocean, and remelting of its crystallization products has produced the huge compositional and isotopic ranges observed in the meteorites.

## 7.2. Relationship between Source Parent/Daughter Ratios and Meteorite Composition

The isotopic systematics of the shergottites demonstrate clear correlations with the incompatible trace element abundances of their whole rocks, such as REE (e.g., Borg et al., 2002), but do not correlate with either major element compositions of the meteorites or the calculated major element compositions of their parental magmas (Herd et al., 2002). These relationships are also evident between the calculated parent/daughter ratios of the sources. For example, the La/Yb ratios of the shergottite bulk rocks correlate with  $^{87}\text{Rb}/^{86}\text{Sr}$  ( $R^2 = 0.86$ ),  $^{147}\text{Sm}/^{144}\text{Nd}$  ( $R^2 = 0.80$ ) and  $^{176}\text{Lu}/^{177}\text{Hf}$  ( $R^2 = 0.96$ ) calculated for the source regions (Table 3). Note that bulk rock La/Yb ratios of the nakhlites fall substantially off the trends defined by the shergottites, most likely reflecting a recent LREE enrichment of their sources. In contrast to bulk rock La/Yb ratios, the Mg# of the parental magmas demonstrate little correlation ( $R^2 = 0.05\text{--}0.23$ ) with  $^{87}\text{Rb}/^{86}\text{Sr}$ ,  $^{147}\text{Sm}/^{144}\text{Nd}$ , and  $^{176}\text{Lu}/^{177}\text{Hf}$  ratios of the sources.

The large range of source compositions calculated for the martian meteorites is unlikely to be produced by interactions between depleted mantle melts and highly differentiated siliceous crust, because all of the martian meteorite parental magmas are basaltic in composition (e.g., Longhi and Pan, 1989).

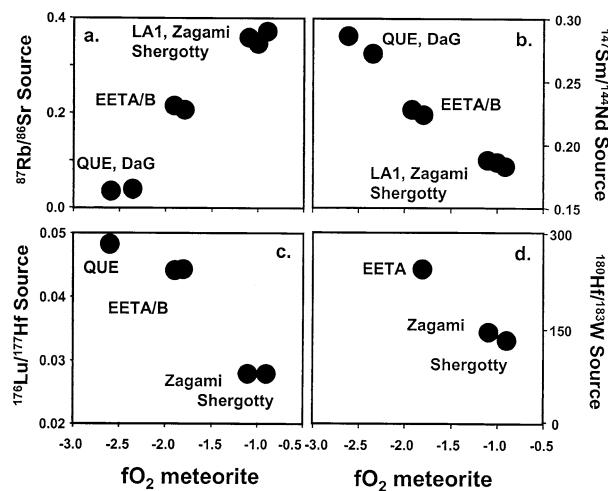


Fig. 8. Plot of  $f_{\text{O}_2}$  estimated by Herd et al. (2001, 2002) for the martian magmas against parent/daughter ratios estimated in this study. Good correlations suggest that the variations in  $f_{\text{O}_2}$  reflect melting sources with variable proportions of a hydrous KREEP-like component.

The decoupling of major element compositions from incompatible trace element and isotopic compositions constrains the mechanisms required to produce the compositional variations inferred for the source regions. If, for example, the variations in trace element and isotopic compositions reflected assimilation of compositionally evolved crustal material by primitive magmas after leaving the mantle, correlations between major element, trace element, and isotopic compositions are expected. This stems from the fact that the trace element and isotopic compositions are controlled by the amount of assimilation, which in turn is controlled by the amount of crystallization of the parental magma.

The lack of correlation between major element compositions of the parental magmas and trace element and isotopic compositions, combined with the fact that the parental magmas of the martian meteorites are basaltic in composition suggests that compositional variations are not controlled by processes in the martian crust. Instead, it is possible that the major element compositions of the parental magmas are limited to some extent by partial melting reactions in the mantle. In this scenario, the trace element and isotopic compositions of the meteorites reflect the compositional range of sources present in the zone of melting, whereas the major element compositions are controlled by eutectic melting processes. Compositional differences between the parental magmas would therefore result primarily from differentiation by fractional crystallization in a closed system, as suggested for QUE by McSween et al. (1996) and for DaG by Wadhwa et al. (2001), after leaving their source regions.

Wadhwa (2001) and Herd et al. (2002) have shown that the  $f_{\text{O}_2}$  estimates for the shergottites correlate with their initial Sr and Nd isotopic compositions. These variations were attributed to addition of a water-rich component to magmas derived from depleted mantle sources. Figure 8 demonstrates that the  $f_{\text{O}_2}$  also correlates with the calculated parent/daughter ratios of the sources regions. This suggests that  $f_{\text{O}_2}$  is controlled by source

Table 4. Partition coefficients used in trace element models.<sup>a</sup>

	Rb	Sr	Sm	Nd	Lu	Hf
Olivine	0.00018	0.00019	0.0043	0.0024	0.0039	0.011
Orthopyroxene	0.0006	0.007	0.012	0.0077	0.065	0.012
Clinopyroxene	0.0011	0.051	0.29	0.17	0.43	0.24
Amphibole	0.33	0.12	0.76	0.44	0.51	0.73
Garnet	0.0007	0.0011	0.25	0.154	8.05	0.27

<sup>a</sup> Partition coefficients for olivine, pyroxene, and garnet Sm, Nd, Lu, and Hf compiled by Beard et al. (1998). Rubidium and strontium partition coefficients for all minerals and Sr, Sm, Nd, Lu, and Hf in amphibole from McKenzie and O’Nions (1991). Amphibole Rb partition coefficient from Dostal et al. (1983).

variation at the time of partial melting, and not by assimilation of the martian crust, and can account for the fact that major element compositions of the parental magmas do not correlate with  $f_{O_2}$  (Herd et al., 2002). Herd et al. (2002) showed that melting and incorporation of a small amount of a hydrous phase, such as amphibole, could strongly alter the  $f_{O_2}$  of highly reduced magmas. Furthermore, a small amount of amphibole is expected to have a relatively minor affect on the trace element and isotopic composition of the parental magma. Thus, the KREEP-like component that is present in the martian meteorite source region could be hydrous. This component must have formed at  $\sim 4.5$  Ga to satisfy the constraints placed on the martian meteorites from their isotopic systematics. Therefore, the hydration of the KREEP-like component inferred to be present in the martian meteorite source region could be associated with early planetary devolatilization.

## 8. FORMATION OF MARTIAN SOURCES AND BASALTIC MAGMAS

### 8.1. Magma Ocean Cumulates

To account for the Sm-Nd and Rb-Sr isotopic systematics of the martian meteorite sources, Borg et al. (1997b) modeled the differentiation of Mars starting at the time of planet formation. In this hypothesis, martian mantle sources were produced by crystallization of a magma ocean and accumulation of minerals. These models follow those of Snyder et al. (1992), but employ a crystallization sequence that is appropriate for Mars: (1)

0–40% crystallization (PCS) 100% olivine; (2) 40–78 PCS 75% orthopyroxene + 25% olivine, (3) 78–86% PCS 75% clinopyroxene + 25% orthopyroxene, (5) 86–99% PCS 95% clinopyroxene + 5% garnet. This crystallization sequence yields a cumulate pile that has the mineral mode estimated for bulk silicate Mars by Longhi et al. (1992). Trace element abundances and ratios in the various mantle cumulates were calculated using first batch (PCS 0-78), and then fractional (PCS 78-99) crystallization models assuming that Mars initially had 2x chondritic abundances of Sr, Sm, Nd, Lu and Hf. In the model presented here, Mars is assumed to have an  $^{87}\text{Rb}/^{86}\text{Sr}$  ratio of 0.16. The partition coefficients used in the models are presented in Table 4. The olivine, pyroxene, and garnet partition coefficients for Sm, Nd, Lu, and Hf are from Beard et al. (1998) who completed an extensive literature search and compiled a set of coefficients that are appropriate to model Sm/Nd and Lu/Hf fractionation in a lunar magma ocean. With the exception of Rb in amphibole, all other partition coefficients used in the models are from a single source (McKenzie and O’Nions, 1991) so as to insure a consistent set of coefficients. The compositional range observed in the martian meteorite sources is modeled as mixing between these depleted mafic cumulates and liquids trapped in the cumulate pile during crystallization. As a result, the compositions of trapped liquids are also calculated in this model.

The  $^{87}\text{Rb}/^{86}\text{Sr}$ ,  $^{147}\text{Sm}/^{144}\text{Nd}$ , and  $^{176}\text{Lu}/^{177}\text{Hf}$  ratios calculated for the various mafic cumulates, trapped liquid, and selected martian meteorite source regions are presented in

Table 5. Parent/daughter ratios of modeled magma ocean cumulates and meteorite sources.<sup>a</sup>

Cumulate or source	Mode	$^{87}\text{Rb}/^{86}\text{Sr}$	$^{147}\text{Sm}/^{144}\text{Nd}$	$^{176}\text{Lu}/^{177}\text{Hf}$
Magma ocean cumulates				
0–40% PCS	ol = 100	0.16	0.590	0.005
40–78% PCS	opx:ol = 75:25	0.029	0.307	0.143
78–86% PCS	cpx:opx = 75:25	0.031	0.308	0.040
86–99% PCS	cpx:grt = 95:5	0.0090	0.271	0.037
Bulk (no amph) cumulates	ol:opx:cpx:grt = 50.2:30.8:18:3.0.7	0.0092	0.285	0.048
Bulk (amph) cumulates	ol:opx:cpx:grt:amph = 49.8:30.41:18:3.0.7:0.8	0.034	0.284	0.046
QUE source		0.036	0.285	0.048
Shergotty source		0.0374	0.182	0.028
Modeled trapped liquid		0.494	0.157	0.014
Lunar KREEP (Rb $\times \sim 2$ )		0.520	0.172	0.014

<sup>a</sup> Longhi et al. (1992) mode bulk Mars ol:opx:cpx:grt = 49.4:31.5:18.8:0.3. PCS = percent crystallization of magma ocean. Modeled trapped liquid = 99% PCS.

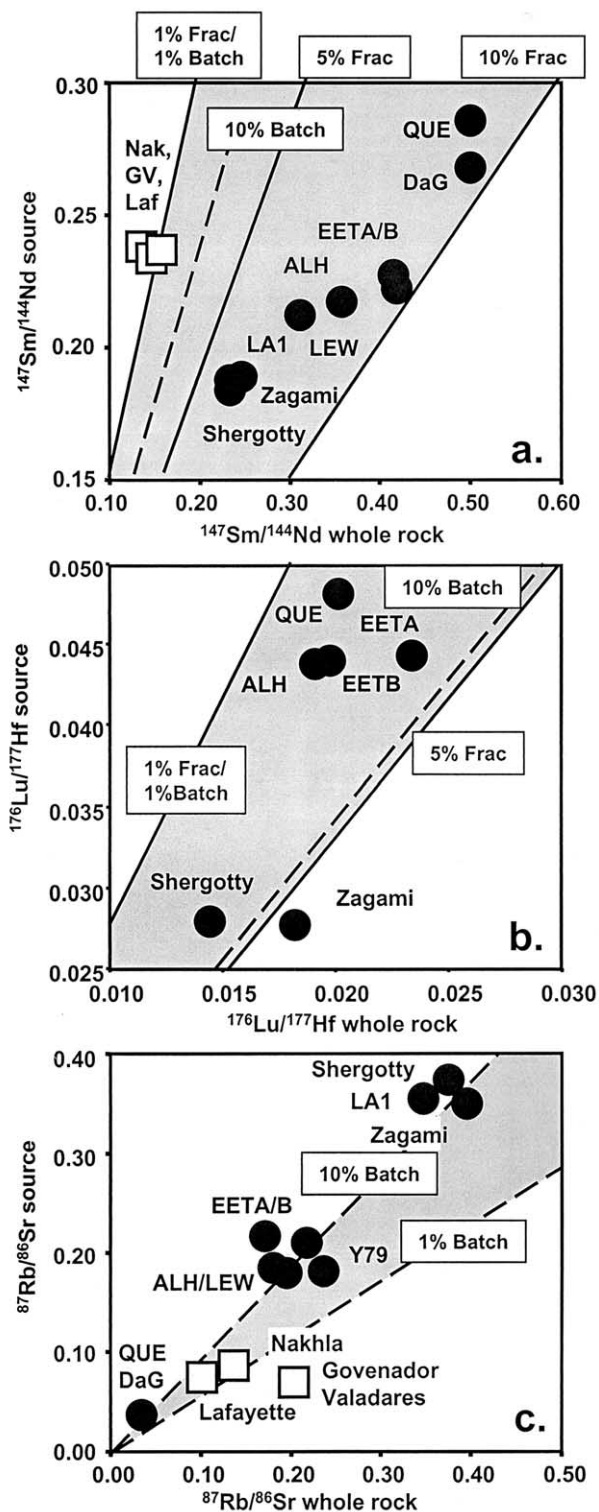


Table 5. Many of the cumulates, including the bulk cumulates, have  $^{147}\text{Sm}/^{144}\text{Nd}$ , and  $^{176}\text{Lu}/^{177}\text{Hf}$  ratios that closely approximate the QUE source region, suggesting that cumulate formation in a magma ocean can account for the Nd and Hf isotopic systematics of the most depleted martian meteorite sources.

Fig. 9. Plots of parent/daughter ratios estimated for the martian meteorite source regions versus whole rock parent/daughter ratios. Symbols are the same as in Figure 5. The shergottites have  $^{147}\text{Sm}/^{144}\text{Nd}$  ratios that are significantly higher than the  $^{147}\text{Sm}/^{144}\text{Nd}$  ratios calculated for their source regions. The nakhlites have  $^{147}\text{Sm}/^{144}\text{Nd}$  ratios that are lower than those calculated for their sources, consistent with a recent LREE-enrichment event in their source regions (see text). In contrast to the Sm-Nd systematics, the shergottites have  $^{176}\text{Lu}/^{177}\text{Hf}$  ratios that are lower than the  $^{176}\text{Lu}/^{177}\text{Hf}$  ratios calculated for their source regions, whereas the  $^{87}\text{Rb}/^{86}\text{Sr}$  ratios of the martian meteorites are roughly the same as those calculated for the shergottite source regions. Dashed lines are modal batch melting models calculated assuming a modal mineralogy in the source of olivine:orthopyroxene:clinopyroxene:garnet = 50.2:30.8:18.3:0.7 and the partition coefficients presented in Table 4. Solid lines are modal fractional partial melting models. Note that neither the batch nor the fractional partial melting models can reproduce the whole rock compositions of the meteorites suggesting that another process or phase, that has not been considered here, is involved in their petrogenesis.

Note however, that the  $^{87}\text{Rb}/^{86}\text{Sr}$  ratio of many of the cumulates are significantly lower than the ratio calculated for the QUE source region. Borg et al. (1997b) attributed this to a small amount of contamination of the QUE magma by a component with an elevated  $^{87}\text{Rb}/^{86}\text{Sr}$  ratio. An alternative explanation is that the mafic mantle source region contains a phase in which Rb is slightly more compatible. A likely candidate is amphibole, because not only is Rb slightly more compatible in amphibole than in olivine, pyroxene, and garnet, but Sm, Nd, Lu, and Hf are all relatively incompatible. Thus, the  $^{147}\text{Sm}/^{144}\text{Nd}$ , and  $^{176}\text{Lu}/^{177}\text{Hf}$  systematics of the modeled cumulates are not strongly affected by its presence. The models demonstrate that addition of ~1% amphibole to the cumulate pile is enough to yield  $^{87}\text{Rb}/^{86}\text{Sr}$  ratios that are similar to those calculated for the QUE source (Table 5). Larger proportions of amphibole in the cumulate pile can produce sources with even higher  $^{87}\text{Rb}/^{86}\text{Sr}$  ratios. Thus, the high  $^{87}\text{Rb}/^{86}\text{Sr}$  source region postulated for EETA/B based on the mixing relationships in Figure 7a may be produced by formation of a mafic cumulate with an even greater proportion of amphibole. To generate a source with a  $^{87}\text{Rb}/^{86}\text{Sr}$  of 0.2 and a  $^{147}\text{Sm}/^{144}\text{Nd}$  of 0.27, the values required for EETA/B by the mixing model (Fig. 7a), the cumulate pile must contain ~5% amphibole. Note that these calculations assume Rb partition coefficients that are typical of hornblende or pargasite and that significantly lower amounts of amphibole would likely be required if a more K-rich amphibole is present. It is therefore possible that the compositional differences between the mafic martian meteorite sources are produced by slight variations in their amphibole modes.

The models also calculate the composition of liquid trapped in the cumulate pile after 99% crystallization of the magma ocean. The composition calculated for the trapped liquid is very similar to the composition of lunar KREEP adjusted for ~2 times higher abundances of Rb. Also note that the composition of the Shergotty source is intermediate between the composition of the martian cumulates and the modeled trapped liquid. Thus, there appears to be at least three mantle sources for the martian meteorites; two derived by accumulation of mafic phases, and possibly characterized by variable amphibole modes, and one representing late stage liquid trapped in the cumulate pile during crystallization of the magma ocean.

## 8.2. Generation of Martian Magmas by Melting of Magma Ocean Cumulates

The  $^{147}\text{Sm}/^{144}\text{Nd}$  ratios estimated for the source regions of the martian meteorites are significantly lower than their whole rock values (Fig. 9a). In contrast, the  $^{176}\text{Lu}/^{177}\text{Hf}$  ratios estimated for the source regions are higher than those observed in the whole rocks (Fig. 9b), whereas the  $^{87}\text{Rb}/^{86}\text{Sr}$  ratios calculated in the sources roughly approximate the ratios observed in the whole rocks (Fig. 9c). The differences between the  $^{147}\text{Sm}/^{144}\text{Nd}$  and  $^{176}\text{Lu}/^{177}\text{Hf}$  ratios of the sources and those of the whole rocks are unlikely to reflect that fact that most of the martian meteorites are cumulates and have undergone some degree of fractional crystallization. This stems from the fact that most of these elements behave incompatibly during crystallization of the major minerals on the liquid line of descent (i.e., crystallization of olivine, pyroxene, and plagioclase. Although the REEs are highly compatible in the phosphates, these are late stage minerals that are unlikely to have either accumulated in, or fractionated from, the bulk rocks. Furthermore, low Al and the absence of large Eu anomalies in the bulk rocks (Fig. 1) confirms that significant amounts of plagioclase fractionation has not occurred. Thus, the whole rock Sm/Nd, Lu/Hf, and Rb/Sr ratios are likely to approximate the ratios of the parental magmas.

The fact that parent/daughter ratios of the meteorite sources, calculated from their isotopic compositions, differ from the parent/daughter ratios of their whole rocks suggests that these ratios were either fractionated in the source region just before generation of the magmas or during the melting processes that produced the parental magmas of the meteorites. Borg et al. (1997b) were able to model the  $^{147}\text{Sm}/^{144}\text{Nd}$  ratio of the QUE whole rock from a source region with a lower  $^{147}\text{Sm}/^{144}\text{Nd}$  ratio by depleting the mantle source region via numerous non-modal batch partial melting events just before the formation of QUE. This required 4 small fraction melting events to change the  $^{147}\text{Sm}/^{144}\text{Nd}$  ratio of the source from 0.285 to  $>0.503$  (the whole rock value for QUE). Applying the same approach to the Lu-Hf systematics of QUE fails, because Hf abundances in the calculated melt are too low. Ultimately, this stems from the fact that the  $^{176}\text{Lu}/^{177}\text{Hf}$  ratio calculated for the source regions are higher than the  $^{176}\text{Lu}/^{177}\text{Hf}$  ratios observed in the whole rocks. Modeled melts generated from QUE-like sources that have undergone multiple episodes of melting have low Hf abundances (e.g.,  $\sim 0.39$  ppm), and high  $^{176}\text{Lu}/^{177}\text{Hf}$  ratios (e.g.,  $\sim 0.07$ ), compared to QUE which has Hf = 3.5 ppm and  $^{176}\text{Lu}/^{177}\text{Hf}$  ratio = 0.02. To yield a melt with a higher Hf abundance, Hf must behave more compatibly during melting. At the same time the Sm-Nd and Rb-Sr systematics of the system cannot be altered dramatically. Thus, a phase characterized by low  $D$ 's for Sm, Nd, Rb, Sr, and Lu, but a high  $D$  for Hf is required. Although ilmenite satisfies these criteria (McKay and Le, 1999) exceedingly large amounts are required to dramatically affect the outcome of the models. Therefore, the inability of these models to reproduce the Rb-Sr, Sm-Nd and Lu-Hf elemental abundances and ratios of the whole rocks suggests that it is unlikely that the martian mantle was depleted as a result of multiple melting events just before the formation of the shergottite parental magma.

Another set of partial melting models are presented in Figure

9. In these figures the parent daughter ratios calculated for the martian meteorite sources based on their initial Sr, Nd, and Hf isotopic compositions are plotted against their whole rock parent/daughter ratios. As discussed above, variations in the parent/daughter ratio calculated for the sources are produced by mixing between depleted and enriched mantle components. Modal fractional (solid lines) and modal batch melting (dashed lines) models are also presented on these figures. The models assume the bulk mineralogy for Mars estimated by Longhi et al. (1992). As a result, a small amount of garnet is present in the mantle source region. From Figure 9 it is apparent that these batch melting models are consistent with the previous batch melting models discussed above and are unable to reproduce both the  $^{147}\text{Sm}/^{144}\text{Nd}$  and  $^{176}\text{Lu}/^{177}\text{Hf}$  ratios of the martian meteorites. The fractional melting models, however, are able to reproduce both the  $^{147}\text{Sm}/^{144}\text{Nd}$  and  $^{176}\text{Lu}/^{177}\text{Hf}$  ratios of the martian meteorites. This stems from the ability of garnet to strongly fractionate the Lu/Hf ratio of the modeled melts, but not strongly fractionate their Sm/Nd ratios. However the fractional melting models are unable to reproduce the  $^{87}\text{Rb}/^{86}\text{Sr}$  ratios of the whole rocks because they fractionated Rb from Sr too efficiently. Furthermore, fractional melting is expected to result in extreme fractionation of highly incompatible elements (e.g., Rb, LREE) from moderately incompatible elements (e.g., Hf, HREE), which is not observed in the meteorite whole rocks. It therefore seems unlikely that simple partial melting can account for the differences between the parent/daughter ratios of the source regions and whole rocks unless: (1) the source region underwent a metasomatic event before melting, (2) the partition coefficients used in the models are incorrect, and/or (3) a phase(s) is present in the mantle source region that has not been considered in the models. These possibilities need to be considered in more detail before the detailed petrogenesis of the martian meteorites can be understood.

## 9. CONCLUSION

Isotopic analysis of the basaltic shergottite DaG 476 yields a Sm-Nd age of  $474 \pm 11$  Ma with an initial  $\varepsilon_{\text{Nd}}^{143}$  value of  $+36.6 \pm 0.8$ . Differences between the age reported here and the age of  $726 \pm 27$  Ma reported by Jagoutz et al. (1999) are attributed to contamination of leachates by Sm-Nd derived from Saharan soils and rocks. Although the Rb-Sr isotopic system has been disturbed, and yields no age information, an initial  $^{87}\text{Rb}/^{86}\text{Sr}$  ratio of  $0.701249 \pm 33$  is estimated from the plagioclase mineral separate using the Sm-Nd age. The initial Sr and Nd isotopic compositions of DaG are most similar to those of the basaltic shergottite QUE. Like QUE, DaG has a strongly LREE-depleted REE pattern indicating that these meteorites have trace element and isotopic compositions that are representative of depleted martian mantle sources. However, the fact that the DaG minerals, whole rock, and parental magma compositions are considerably more mafic than QUE, suggests that the apparent decoupling of major element abundances from trace element abundances and isotopic compositions may result from differentiation of the martian magmas in a closed system by fractional crystallization after leaving the source region.

The age of mantle source formation is calculated using a two-stage model isochron based on measured whole rock  $\varepsilon_{\text{Nd}}^{142}$  and initial  $\varepsilon_{\text{Nd}}^{143}$  values of the martian meteorites to be 4.513 Ga.

This age is only valid as long as the sources of the meteorites had a relatively simple two-stage evolutionary history. Several meteorites fall off this isochron, including the nakhlites and Chassigny. The source region of these meteorites is interpreted to have undergone multi-stage evolution that involved a relatively recent LREE-enrichment event. This is consistent with the fact that these meteorites have positive initial  $\epsilon_{\text{Nd}}^{143}$  values, but flat chondrite-normalized REE patterns. The  $^{87}\text{Rb}/^{86}\text{Sr}$ ,  $^{147}\text{Sm}/^{144}\text{Nd}$ , and  $^{176}\text{Lu}/^{177}\text{Hf}$  ratios calculated for the source regions of the meteorites from their initial Sr, Nd, and Hf isotopic ratios, correlate. Therefore, these parent/daughter ratios were probably fractionated in silicate reservoirs on Mars during early planetary differentiation. Mixing models demonstrate that the variability observed in parent/daughter ratios of the martian meteorites can be produced by interactions of martian sources with the characteristics similar to depleted lunar mantle and KREEP. Much of the compositional variability observed in the martian meteorites could reflect interactions of source regions produced by crystallization of a magma ocean, and does not require differentiation to have occurred in the martian crust. Mixing models also demonstrate that at least three source regions are required to produce the isotopic variability calculated for the martian meteorites. The composition of two of the sources can be modeled as mafic cumulates crystallizing from a magma ocean with variable proportions of a phase in which Rb is slightly compatible (amphibole?), whereas the third source has the characteristics of liquids trapped in the cumulate pile during crystallization.

*Acknowledgments*—We wish to thank B. Beard and an anonymous reviewer for helpful reviews. Discussions and commentary with C. Shearer, J. Papike, and Y. Asmerom helped to refine many ideas presented in this manuscript. This work was supported by NASA grant NAG9-1111.

*Associate editor:* C. R. Neal

## REFERENCES

- Anders E. and Grevesse N. (1989) Abundances of the elements: Meteoritic and solar. *Geochim. Cosmochim. Acta* **53**, 197–214.
- Banin A., Clark B. C., and Wänke H. (1992) Surface chemistry and mineralogy. In *Mars* (eds. H. Kieffer et al.), pp. 594–625. University of Arizona Press.
- Beard B. L., Taylor L. E., Scherer E. E., Johnson C. M., and Snyder G. A. (1998) The source region and melting mineralogy of high-titanium and low-titanium lunar basalts deduced from Lu-Hf isotope data. *Geochim. Cosmochim. Acta* **62**, 525–544.
- Begemann F., Ludwig K. R., Lugmair G. W., Min K., Nyquist L. E., Patchett P. J., Renne P. R., Shih C.-Y., Villa I. M., and Walker R. J. (2001) Call for an improved set of decay constants for geochronological use. *Geochim. Cosmochim. Acta* **65**, 111–121.
- Blichert-Toft J. and Albarède F. (1997) The Lu-Hf isotope geochemistry of chondrites and the evolution of the crust–mantle system. *Earth Planet. Sci. Lett.* **154**, 243–258.
- Blichert-Toft J., Gleason J. D., Tétlock P., and Albarède F. (1999) The Lu-Hf isotope geochemistry of shergottites and the evolution of the martian mantle–crust system. *Earth Planet. Sci. Lett.* **173**, 25–39.
- Borg L. E., Nyquist L. E., Wiesmann H., and Shih C.-Y. (1997a) Rb-Sr and Sm-Nd isotopic analysis of QUE 94201: Constraints on martian differentiation (abstract). *Lunar Planet. Sci. Conf.* **28**, 133–134.
- Borg L. E., Nyquist L. E., Wiesmann H., and Shih C.-Y. (1997b) Constraints on Martian differentiation processes from Rb-Sr and Sm-Nd isotopic analyses of the basaltic shergottite QUE94201. *Geochim. Cosmochim. Acta* **61**, 4915–4931.
- Borg L. E., Nyquist L. E., Reese Y., and Wiesmann H. (2002) Constraints on the petrogenesis of martian meteorites from the partially disturbed Rb-Sr and Sm-Nd isotopic systematics of LEW88516 and ALH77005. *Geochim. Cosmochim. Acta* **66**, 2037–2053.
- Brandon A. D., Walker R. J., Morgan J. W., and Goles G. G. (2000) Re-Os isotopic evidence for early differentiation of the martian mantle. *Geochim. Cosmochim. Acta* **64**, 4038–4095.
- Burghel A., Dreibus G., Palme H., Rammensee W., Spettel B., Weckwerth G., and Wänke H. (1983) Chemistry of shergottites and the shergottite parent body (SPB): Further evidence for the two component model for planet formation (abstract). *Lunar Planet. Sci. Conf.* **14**, 80–81.
- Chen J. H. and Wasserburg G. J. (1986) Formation ages and evolution of Shergotty and its parent planet from U-Th-Pb systematics. *Geochim. Cosmochim. Acta* **50**, 955–968.
- Crozaz G. and Wadhwa M. (2001) The terrestrial alteration of Saharan shergottites Dar al Gani 476 and 489: A case study of weathering in a hot desert environment. *Geochim. Cosmochim. Acta* **65**, 971–978.
- Dostal J., Dupuy C., Carron J. P., LeGuen de Kerneizon M., and Maury R. C. (1983) Partition coefficients of trace elements: Application to volcanic rocks of St. Vincent, West Indies. *Geochim. Cosmochim. Acta* **47**, 525–533.
- Dreibus G. and Wänke H. (1985) Mars: A volatile-rich planet. *Meteor. Planet. Sci.* **20**, 367–380.
- Dreibus G., Jochum K. H., Palme H., Spettel B., Wlotzka F., and Wänke H. (1992) LEW88516: A meteorite compositionally close to the “martian mantle” (abstract). *Meteor. Planet. Sci.* **27**, 216–217.
- Dreibus G., Spettel B., Wlotzka F., Schultz L., Weber H. W., Jochum K., and Wänke H. (1996) QUE94201: An unusual martian basalt (abstract). *Meteor. Planet. Sci.* **31**, A39–A40.
- Dreibus G., Spettel B., Haubold R., Jochum K. P., Palme H., Wolf D., and Zipfel J. (2000) Chemistry of a new shergottite: Sayh al Uhaymir 005 (abstract). *Meteor. Planet. Sci.* **35**, A49.
- Edmunson J., Borg L. E., Shearer C., Papike J. J., and Davidson K. (2001) High Si-glasses in basaltic shergottite DaG 476 and their implications for geochronology (abstract). *Lunar Planet. Sci. Conf.* **32**, 1439 (CD-ROM).
- Gale N. H. (1975) The chronology of the Nakhla achondrite meteorite. *Earth Planet. Sci. Lett.* **26**, 195–206.
- Grousset F. E., Biscaye P. E., Zindler A., Prospero J., and Chester R. (1988) Neodymium isotopes as tracers in marine sediments and aerosols: North Atlantic. *Earth Planet. Sci. Lett.* **87**, 367–378.
- Halliday A. N., Wänke H., Birck J.-L., and Clayton R. N. (2001) The accretion, composition and early differentiation of Mars. *Space Sci. Rev.* **96**, 197–230.
- Harper C. L., Nyquist L. E., Bansal B., Wiesmann H., and Shih C.-Y. (1995) Rapid accretion and early differentiation of Mars indicated by  $^{142}\text{Nd}/^{144}\text{Nd}$  in SNC meteorites. *Science* **267**, 213–217.
- Harper C. L. and Jacobsen S. B. (1996) Evidence for  $^{182}\text{Hf}$  in the early Solar System and constraints on the timescale of terrestrial accretion and core formation. *Geochim. Cosmochim. Acta* **60**, 1131–1154.
- Harvey R. P., Wadhwa M., McSween H. Y. Jr., and Crozaz G. (1993) Petrology, mineral chemistry, and petrogenesis of Antarctic shergottite LEW88516. *Geochim. Cosmochim. Acta* **57**, 4769–4783.
- Herd C. D. K., Papike J. J., and Breyar A. J. (2001) Oxygen fugacity of martian basalts from electron microprobe oxygen and TEM-EELS analyses of Fe-Ti oxides. *Am. Mineral.* **86**, 1015–1024.
- Herd C. D. K., Borg L. E., and Papike J. J. (2002) Systematics of oxygen fugacity and geochemical variations in the martian basalts: Implications for martian basalt petrogenesis and oxidation state of the upper mantle of Mars. *Geochim. Cosmochim. Acta* **66**, 2025–2036.
- Ireland T. R., Kirby H., Bukovanska M., and Wlotzka F. (2000) Hf-W systematics of meteoritic zircon revisited (abstract). *Lunar Planet. Sci. Conf.* **31**, 1540 (CD-ROM).
- Jagoutz E. (1991) Chronology of SNC meteorites. *Space Sci. Rev.* **56**, 13–22.
- Jagoutz E. (1996) Nd isotopic systematics of Chassigny (abstract). *Lunar Planet. Sci. Conf.* **27**, 597–598.
- Jagoutz E., Palme H., Baddenhausen H., Blum K., Cendales M., Dreibus G., Spettel B., Lorenz V., and Wänke H. (1979) The abundances of major, minor, and trace elements in the Earth’s mantle

- as derived from primitive ultramafic nodules. *Proc. Lunar Planet. Sci. Conf.* **10**, 2031–2050.
- Jagoutz E., Bogdanovski O., Krestina N., and Jotter R. (1999) DaG: A new age in the SNC family or the first gathering of relatives (abstract). *Lunar Planet. Sci. Conf.* **30**, 1808 (CD-ROM).
- Jones J. H. (1989) Isotopic relationships among the Shergottites, Nakhilites and Chassigny. *Proc. Lunar Planet. Sci. Conf.* **19**, 465–474.
- Kleine T., Münker C., Mezger K., and Palme H. (2002) Rapid accretion and early core formation on asteroids and the terrestrial planets from Hf-W chronometry. *Nature* **481**, 952–954.
- Lee D.-C. and Halliday A. N. (1997) Rapid accretion and early core formation on asteroids and the terrestrial planets from Hf-W chronometry. *Nature* **418**, 952–955.
- Longhi J. (1991) Complex magmatic processes on Mars: Inferences from SNC meteorites. *Proc. Lunar Planet. Sci. Conf.* **21**, 465–475.
- Longhi J. and Pan V. (1989) The parent magmas of the SNC meteorites. *Proc. Lunar Planet. Sci. Conf.* **19**, 451–464.
- Longhi J., Knittle E., Holloway J. R., and Wänke H. (1992) The bulk composition, mineralogy, and internal structure of Mars. In *Mars* (eds. H. Kieffer et al.), pp. 184–208. University of Arizona Press.
- Lugmair G. W. and Galer S. J. G. (1992) Age and isotopic relations among angrites Lewis Cliff 86010 and Angra dos Reis. *Geochim. Cosmochim. Acta* **56**, 1673–1694.
- Ma M. S., Laul J. C., and Schmitt R. A. (1982) Complementary rare earth element patterns in unique achondrites, such as ALHA79001 and shergottites, and in the Earth. *Proc. Lunar Planet. Sci. Conf.* **12**, 1349–1358.
- McKay G. A. and Le L. (1999) Partitioning of tungsten and hafnium between ilmenite and mare basalt melt (abstract). *Lunar Planet. Sci. Conf.* **30**, 1996 (CD-ROM).
- McKenzie D. and O’Nions R. K. (1991) Partial melt distributions from inversion of rare earth element concentrations. *J. Petrol.* **32**, 1021–1091.
- McSween H. Y. Jr. (1994) What have we learned about Mars from SNC meteorites. *Meteor. Planet. Sci.* **29**, 757–779.
- McSween H. Y. Jr., Lundburg L., and Crozaz G. (1988) Crystallization of ALH77005 shergottite: How closed is a closed system? (abstract). *Lunar Planet. Sci. Conf.* **19**, 766–767.
- McSween H. Y. Jr., Eisenhour D. D., Taylor L. A., Wadhwa M., and Crozaz G. (1996) QUE94201 shergottite: Crystallization of a Martian basaltic magma. *Geochim. Cosmochim. Acta* **60**, 4563–4569.
- Mikouchi T. (1999) Preliminary examination of Dar al Gani 476: A new martian meteorite similar to lithology A of EET79001 (abstract). *Lunar Planet. Sci. Conf.* **30**, 1557 (CD-ROM).
- Mikouchi T., Miyamoto M., and McKay G. A. (2001) Mineralogy and petrology of the Dar al Gani martian meteorite: Implications for its cooling history and relationship to other shergottites. *Meteor. Planet. Sci.* **36**, 531–548.
- Misawa K., Nakamura N., Premo W. R., and Tatsumoto M. (1997) U-Th-Pb isotopic systematics of lherzolitic shergottite Yamato-793605. *Antarct. Meteor. Res.* **10**, 95–108.
- Mittlefehldt D. W., Wentworth S. J., Wang M.-S., Lindstrom M. M., and Lipschutz M. E. (1997) Geochemistry of alteration phases in martian lherzolite Y-793605. *Antarct. Meteor. Res.* **10**, 109–124.
- Morikawa N., Misawa K., Kondoroski G., Premo W. R., Tatsumoto M., and Nakamura N. (2001) Rb-Sr isotopic systematics of lherzolitic shergottite Yamato-793605. *Antarct. Meteor. Res.* **14**, 47–60.
- Nakamura N., Unruh D. M., Tatsumoto M., and Hutchison R. (1982a) Origin and evolution of the Nakhla meteorite inferred from Sm-Nd and U-Pb systematics and REE, Ba, Sr, Rb abundances. *Geochim. Cosmochim. Acta* **46**, 1555–1573.
- Nakamura N., Komi K., and Kagami H. (1982b) Rb-Sr isotopic and REE abundances in the Chassigny meteorite (abstract). *Meteor. Planet. Sci.* **17**, 257–258.
- Neal C. R. (2001) Interior of the Moon: The presence of garnet in the primitive deep lunar mantle. *J. Geophys. Res.* **106**, 27865–27885.
- Nyquist L. E. (1977) Lunar Rb-Sr chronology. *Phys. Chem. Earth.* **10**, 103–142.
- Nyquist L. E., Wooden J., Bansal B., Wiesmann H., McKay G. A., and Bogard D. D. (1979) Rb-Sr age of Shergotty achondrite and implications for metamorphic resetting of isochron ages. *Geochim. Cosmochim. Acta* **43**, 1057–1074.
- Nyquist L. E. and Shih C.-Y. (1992) The isotopic record of lunar volcanism. *Geochim. Cosmochim. Acta* **56**, 2213–2234.
- Nyquist L. E., Bansal B. M., Wiesmann H., and Shih C.-Y. (1995) “Martians” young and old: Zagami and ALH84001 (abstract). *Lunar Planet. Sci. Conf.* **26**, 1065–1066.
- Nyquist L. E., Reese Y. D., Wiesmann H., and Shih C.-Y. (2000) Rubidium-strontium age of Los Angeles shergottite (abstract). *Meteor. Planet. Sci.* **35**, A121–A122.
- Nyquist L. E., Reese Y., Wiesmann H., and Shih C.-Y. (2001a) Age of EET79001B and implications for shergottite origins (abstract). *Lunar Planet. Sci. Conf.* **32**, 1407 (CD-ROM).
- Nyquist L. E., Bogard D. D., Shih C.-Y., Greshake A., Stoffer D., and Eugster O. (2001b) Ages and histories of martian meteorites. In *Chronology and Evolution of Mars 96* (eds. R. Kalenback, J. Geiss, and W. K. Hartmann), pp. 105–164. Kluwer.
- Paces J. B., Nakai S., Neal C. R., Taylor L. A., Halliday A. N., and Lee D.-C. (1991) A strontium and neodymium isotopic study of Apollo 17 high-Ti mare basalts: Resolution of ages, evolution of magmas, and origins of source heterogeneities. *Geochim. Cosmochim. Acta* **55**, 2025–2043.
- Palme H. and Beer H. (1993) The significance of W in planetary differentiation processes: Evidence from new data on eucrites. *Proc. Lunar Sci. Conf.* **12B**, 949–964.
- Papanastassiou D. A. and Wasserburg G. J. (1974) Evidence for late formation and young metamorphism in the achondrite Nakhla. *Geophys. Res. Lett.* **1**, 23–26.
- Rubin A. E., Warren P. H., Greenwood J. P., Verish R. S., Leshin L. A., Hervig R. L., and Clayton R. N. (2000) Los Angeles. The most differentiated basaltic meteorite. *Geology* **28**, 1011–1014.
- Schaaf P. and Müller-Sohnius D. (2002) Strontium and neodymium isotopic study of Libyan desert glass: Inherited Pan-African age signatures and new evidence for target material. *Meteor. Planet. Sci.* **37**, 565–576.
- Schmitt R. A. and Smith R. H. (1963) Implications of the similarity in rare earth fractionation of the nakhilite meteorites and terrestrial basalts. *Nature* **199**, 550–551.
- Shih C.-Y., Nyquist L. E., Bogard D. D., McKay G. A., Wooden J. L., Bansal B. M., and Wiesmann H. (1982) Chronology and petrogenesis of young achondrites, Shergotty, Zagami, and ALHA 77005: Late magmatism on a geologically active planet. *Geochim. Cosmochim. Acta* **46**, 2323–2344.
- Shih C.-Y., Nyquist L. E., Bansal B. M., and Wiesmann H. (1992) Rb-Sr and Sm-Nd chronology of an Apollo 17 KREEP basalt. *Earth Planet. Sci. Lett.* **108**, 203–215.
- Shih C.-Y., Nyquist L. E., Dasch E. J., Bogard D. D., Bansal B. M., and Wiesmann H. (1993) Age of pristine noritic clasts from lunar breccias 15445 and 15455. *Geochim. Cosmochim. Acta* **57**, 915–931.
- Shih C.-Y., Nyquist L. E., Reese Y., and Wiesmann H. (1998) The chronology of the nakhilite Lafayette: Rb-Sr and Sm-Nd isotopic ages (abstract). *Lunar Planet. Sci. Conf.* **29**, 1145 (CD-ROM).
- Shih C.-Y., Nyquist L. E., and Wiesmann H. (1999) Samarium-neodymium and rubidium-strontium systematics of nakhilite Govenador Valadares. *Meteor. Planet. Sci.* **34**, 647–656.
- Shirey S. B. and Walker R. J. (1998) The Re-Os isotope system in cosmochemistry and high temperature geochemistry. *Annu. Rev. Earth Planet. Sci.* **26**, 423–500.
- Snyder G. A., Taylor L. A., and Neal C. R. (1992) A chemical model for generating the source of mare basalts: Combined equilibrium and fractional crystallization of the lunar magmashpere. *Geochim. Cosmochim. Acta* **56**, 3809–3823.
- Snyder G. A., Lee D.-C., Taylor L. A., Halliday A. N., and Jerde E. A. (1994) Evolution of the upper mantle of the Earth’s Moon: Neodymium and strontium isotopic constraints on high Ti-mare basalts. *Geochim. Cosmochim. Acta* **58**, 4795–4808.
- Snyder G. A., Borg L. E., Nyquist L. E., and Taylor L. A. (2000) Chronology and isotopic constraints on lunar evolution. In *Origin of the Earth and Moon* (eds. R. M. Canup and K. Righter), pp. 361–398. University of Arizona Press.
- Stolper E. and McSween H. Y. Jr. (1979) Petrology and origin of the shergottite meteorites. *Geochim. Cosmochim. Acta* **43**, 589–602.
- Taylor L. A., Nazarov M. A., Shearer C. K., McSween H. Y. Jr., Cahill J., Neal C. R., Ivanova M. A., Barsukova L. D., Lentz R. C., Clayton

- R. N., and Mayeda T. K. (2002) Martian meteorite Dhofar 019: A new shergottite. *Meteor. Planet. Sci.* **37**, 1107–1128.
- Treiman A. H. (1986) The parental magma of the Nakhla achondrite: Ultrabasic volcanism on the shergottite parent body. *Geochim. Cosmochim. Acta* **50**, 1061–1070.
- Unruh D. M., Stille P., Patchett P. J., and Tatsumoto M. (1984) Lu-Hf and Sm-Nd evolution of lunar mare basalts. *Proc. Lunar Planet. Sci. Conf.* **14**, B459–B477.
- Wadhwa M. (2001) Redox state of Mars' upper mantle and crust from Eu anomalies in shergottite pyroxenes. *Science* **291**, 1527–1530.
- Wadhwa M., Lentz R. C. F., McSween H. Y. Jr., and Crozaz G. (2001) A petrologic and trace element study of Dar al Gani 476 and Dar al Gani 489: Twin meteorites with affinities to basaltic and lherzolithic shergottites. *Meteor. Planet. Sci.* **36**, 195–208.
- Walker R. J., Brandon A. D., Nazarov M. A., Mittlefehldt D., and Taylor L. A. (2002)  $^{187}\text{Re}/^{188}\text{Os}$ . Isotopic studies of SNC meteorites: An update (abstract). *Lunar Planet. Sci. Conf.* **33**, 1042 (CD-ROM).
- Wänke H. and Dreibus G. (1988) Chemical composition and accretional history of terrestrial planets. *Phil. Trans. R. Soc. Lond. A* **235**, 545–557.
- Warren P. H. and Wasson J. T. (1979) The origin of KREEP. *Rev. Geophys. Space Phys.* **17**, 73–88.
- Wooden J. L., Nyquist L. E., Bogard D. D., Bansal B. M., Wiesmann H., Shih C.-Y., and McKay G. (1979) Radiometric ages of achondrites Chervony Kut, Governador Valadares, and Allan Hills 77005 (abstract). *Lunar Planet. Sci. Conf.* **10**, 1379–1381.
- Wooden J. L., Shih C.-Y., Nyquist L. E., Bansal B. M., Wiesmann H., and McKay G. (1982) Rb-Sr and Sm-Nd isotopic constraints on the origin of EETA 79001: A second Antarctic shergottite (abstract). *Lunar Planet. Sci. Conf.* **13**, 879–880.
- Yin Q. Z., Jacobsen S. B., Yamashita K., Blichert-Toft J., Télouk P., and Albarède F. (2002) New Hf-W data that are consistent with Mn-Cr chronology: Implications for early solar system evolution (abstract). *Lunar Planet. Sci. Conf.* **33**, 1700 (CD-ROM).
- York D. (1966) Least squares fitting of a straight line. *Can. J. Phys.* **44**, 1079–1086.
- Zipfel J., Scherer P., Spettel B., Dreibus G., and Schultz L. (2000) Petrology and chemistry of the new shergottite Dar al Gani 476. *Meteor. Planet. Sci.* **35**, 95–106.